HYDROFLUIDIC YAW SAS ANALYSIS DESIGN AND DEVELOPMENT

Harvey D. Ogren

Honeywell, Incorporated

Prepared for:

Army Air Mobility Research and Development Laboratory

March 1974

DISCLAIMERS

The findings in this report are not to be construed as an official Department of the Army position unless so designated by other authorized documents.

When Government drawings, specifications, or other data are used for any purpose other than in connection with a definitely related Government procurement operation, the United States Government thereby incurs no responsibility nor any obligation whatsoever; and the fact that the Government may have formulated, furnished, or in any way supplied the said drawings, specifications, or other data is not to be regarded by implication or otherwise as in any manner licensing the holder or any other person or corporation, or conveying any rights or permission, to manufacture, use, or sell any patented invention that may in any way be related thereto.

Trade names cited in this report do not constitute an official endorsement or approval of the use of such commercial hardware or software.

DISPOSITION INSTRUCTIONS

Destroy this report when no longer needed. Do not return it to the originator.

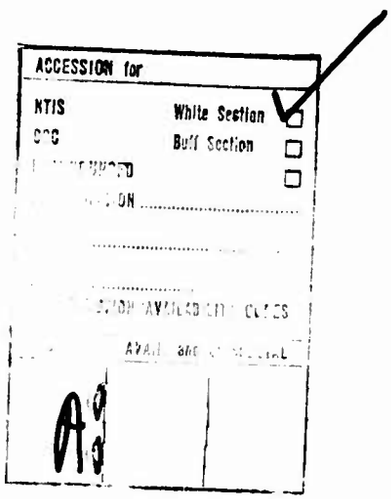

DEPARTMENT OF THE ARMY
US ARMY AIR MOBILITY RESEARCH & DEVELOPMENT LABORATORY
EUSTIS DIRECTORATE
FORT EUSTIS, VIRGINIA 23604

This report has been reviewed by the Eustis Directorate, U.S. Army Air Mobility Research and Development Laboratory and is considered to be technically sound.

The purpose of the program was to design and develop the integrated sensor/controller/series servoactuator package of a hydrofluidic yaw stability augmentation system that will be demonstrated in a subsequent operational suitability test program.

The report is published for the exchange of information and appropriate application. The technical monitor for this program was Mr. George W. Fosdick, Applied Aeronautics technical area, Systems Support Division, Eustis Directorate.

Task 1F162204AA4405
Contract DAAJ02-72-C-0051
USAAMRDL Technical Report 74-7
March 1974

HYDROFLUIDIC YAW SAS ANALYSIS DESIGN AND DEVELOPMENT

Final Report

By
Harvey D. Ogren

Prepared by
Honeywell Inc.
Government and Aeronautical Products Division
Minneapolis, Minnesota

for

EUSTIS DIRECTORATE
U.S. ARMY AIR MOBILITY
RESEARCH AND DEVELOPMENT LABORATORY
FORT EUSTIS, VIRGINIA

Unclassified

Security Classification

AD 777804

DOCUMENT CONTROL DATA - R & D

(Security classification of title, body of abstract and indexing annotation must be entered when the overall report is classified)

1. ORIGINATING ACTIVITY (Corporate author)	2a. REPORT SECURITY CLASSIFICATION
Honeywell Inc., Government and Aeronautical Products Division 1625 Zarthan Ave., Minneapolis, Minn. 55416	Unclassified 2b. GROUP

3. REPORT TITLE

HYDROFLUIDIC YAW SAS ANALYSIS DESIGN AND DEVELOPMENT

4. DESCRIPTIVE NOTES (Type of report and inclusive dates)

Final Report - 1 April 1972 - 1 October 1973

5. AUTHOR(S) (First name, middle initial, last name)

Harvey D. Ogren

6. REPORT DATE	7a. TOTAL NO. OF PAGES	7b. NO. OF REFS
March 1974	62	0

8a. CONTRACT OR GRANT NO	9a. ORIGINATOR'S REPORT NUMBER(S)
DAAJ02-72-C-0051 b. PROJECT NO Task 1F162204AA4405 c d	USAAMRDL Technical Report 74-7 9b. OTHER REPORT NO(S) (Any other numbers that may be assigned this report) WO517-FR

10. DISTRIBUTION STATEMENT

Approved for public release; distribution unlimited.

11. SUPPLEMENTARY NOTES	12. SPONSORING MILITARY ACTIVITY
	Eustis Directorate, U.S. Army Air Mobility, Research and Development Laboratory, Fort Eustis, Virginia

13. ABSTRACT

The objective of this program is to design and develop the integrated sensor/controller/series servoactuator package of a hydrofluidic stability augmentation system which will be subsequently demonstrated during operational suitability tests. The sensor/controller was designed based on the performance of a breadboard model that was flight tested in the OH-58A helicopter. From the flight test program, the system gain was increased and a straight rate loop was added as a result of pilot requests. The final system gain was 0.023 inch of servoactuator per degree per second of rate input. The straight rate loop gain was set at 10 percent of the system gain. Temperature compensation was incorporated into the various circuits by adding negative feedback that contained a viscous resistor. This technique reduced the gain change versus temperature that was obtained in the past. The system was tested at various oil temperatures and vibrated sinusoidally in each axis. During the after-vibration tests the servoactuator ceased to function. It was returned to the vendor for repair. Due to a delay in the vendor's returning the servoactuator, the sensor/controller was adapted to another servoactuator. The system was recalibrated, tested and delivered for flight test in the OH-58A helicopter. The flight test will be reported under Contract DAAJ02-72-C-0111.

DD FORM 1 NOV 68 1473 REPLACES DD FORM 1473, 1 JAN 64, WHICH IS OBSOLETE FOR ARMY USE.

Unclassified

Security Classification

Unclassified

Security Classification

14 KEY WORDS	LINK A		LINK B		LINK C	
	ROLE	WT	ROLE	WT	ROLE	WT
Fluidic						
Stability Augmentation System						
Helicopter						

UNCLASSIFIED

FOREWORD

This document is the final report of a program to analyze, design, and develop a hydrofluidic yaw axis damper system for the OH-58A helicopter. This program was authorized by the Eustis Directorate, U. S. Army Air Mobility Research and Development Laboratory, under Contract DAAJ02-72-C-0051, Task 1F162204AA4405. The technical monitor of this program was Mr. G. W. Fosdick. This program is part of the U. S. Army's continuing effort to develop stability augmentation systems for helicopters. The work presented started 1 April 1972 and was completed 1 October 1973.

TABLE OF CONTENTS

LIST OF ILLUSTRATIONS

LIST OF TABLES

LIST OF SYMBOLS

A	lateral cyclic displacement, inc.
e	2.7314
g	acceleration of gravity, ft/sec^2
$G_{amp\ 1}$	gain amplifier 1, psi/psi
$G_{amp\ 2}$	gain amplifier 2, psi/psi
$G_{amp\ 3}$	gain amplifier 3, psi/psi
$G_{amp\ 4}$	gain amplifier 4, psi/psi
G_{PID}	gain pilot input device, psi/in. of cable
G_{VRS}	gain vortex rate sensor, psi/deg/sec
K_1	gain, psi/psi
$K_{\dot{\phi}}$	roll damper gain, in./rad/sec
K_{δ}	pilot input gain, in./in. of pedal
K_r	yaw damper gain, rad/rad/sec
L	roll moment, ft-lb
N	yaw moment, ft-lb
N_r	yaw rate damping derivative
P	roll rate, rad/sec
R_c	reference pressure, psi
r	yaw axis angular rate, rad/sec

S	Laplace operator
T	time, sec
V	side velocity, ft/sec
v	velocity, ft/sec
v_g	lateral gust, ft/sec
Y	side force, lb
ϕ	roll angle, rad
$\dot{\phi}$	roll angular rate, rad/sec
δ_R	tail rotor displacement, in.
δ_S	yaw servo, in.
η	sensor angle, deg

SECTION I
INTRODUCTION

The yaw axis hydrofluidic stability augmentation system was designed based on data obtained under Contract DAAJ02-72-C-0111, OH-58A Hydrofluidic Yaw Stability Augmentation System Flight Test Program. The servoactuator and sensor/controller were designed so that the sensor/controller mounts directly on the servoactuator and receives its hydraulic power from it. Also, based upon the results of the flight test program, a straight rate loop circuit was added to modify the aircraft characteristics at hover. The controller section incorporated negative feedback and viscous resistors so as to temperature-compensate the amplifier circuits.

This sensor/controller/servoactuator was assembled and evaluated at various temperatures, vibrated, and then retested after vibration. The servoactuator failed to function during the after-vibration tests. The sensor/controller was subsequently connected to another servoactuator and testing completed.

The unit was then installed in an OH-58 helicopter for flight test evaluation.

SECTION II
SYSTEM DESIGN

GENERAL

Previous analytical effort to determine the gains and shaping networks required for a damper system for the directional axis of the OH-58A helicopter was conducted and the equation for a Hydrofluidic Yaw Stability Augmentation System (HYSAS) was determined. This is shown in Figures 1 and 2, with the curve of phase angle and gain change versus frequency. The block diagram to obtain this performance is shown in Figure 3.

To improve the temperature operating range capability of the system, a technique using negative feedback around each amplifier circuit was incorporated into the system. The temperature compensation comes from the use of a temperature-sensitive resistor in the feedback loop (described in detail in this report).

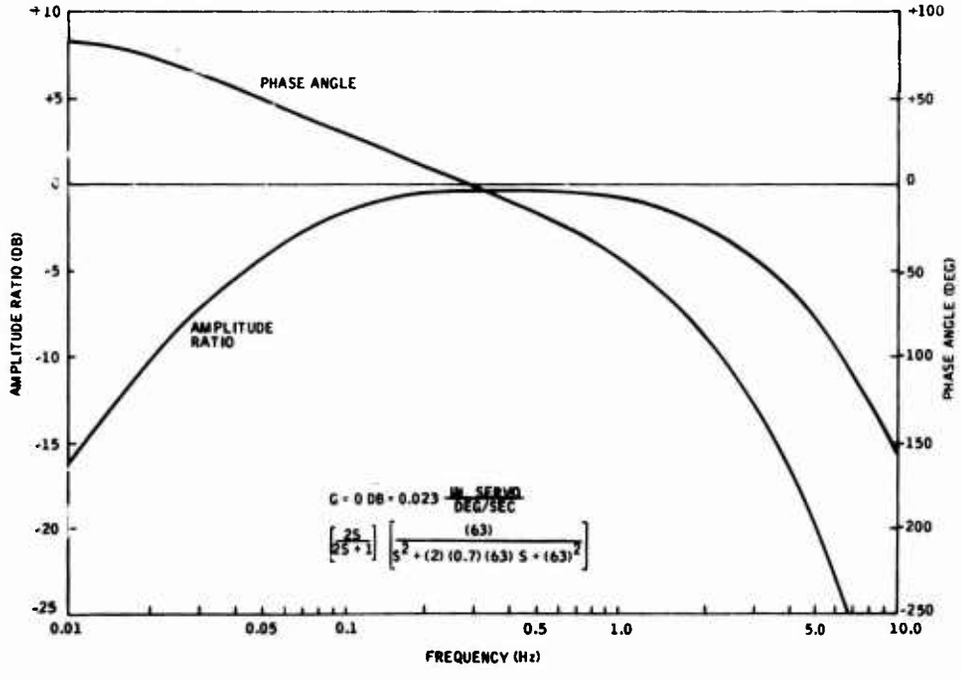

Figure 1. Rate Transfer Function.

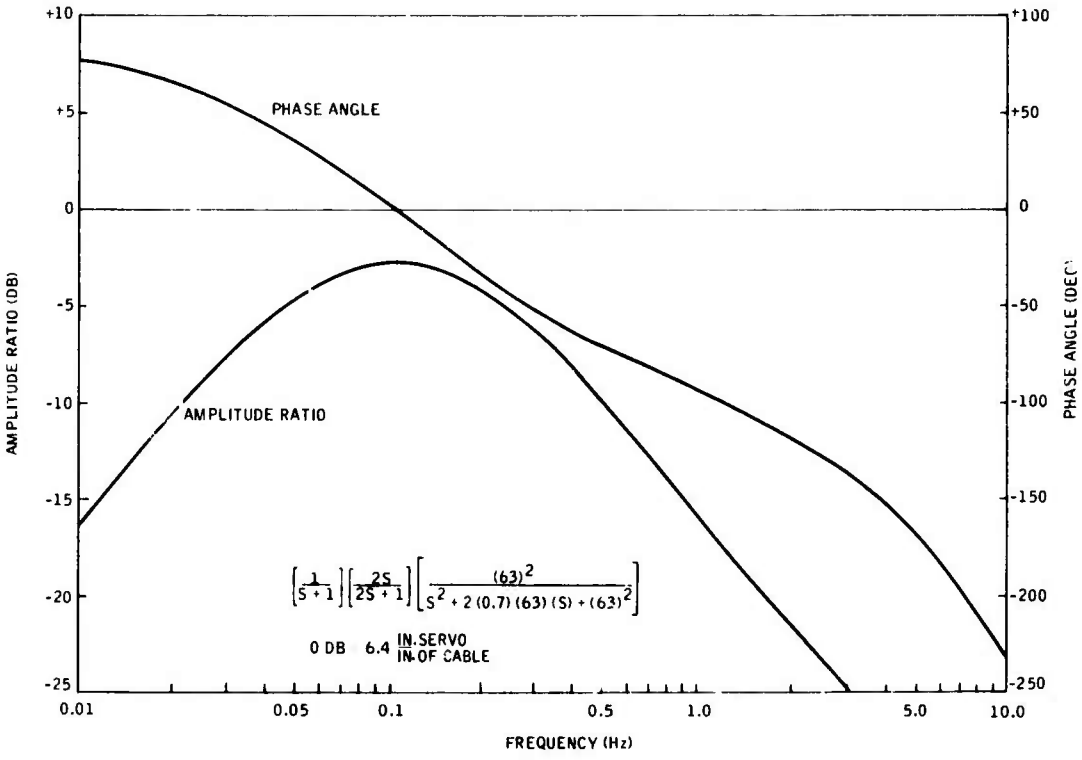

Figure 2. Pilot Input Transducer Transfer Function.

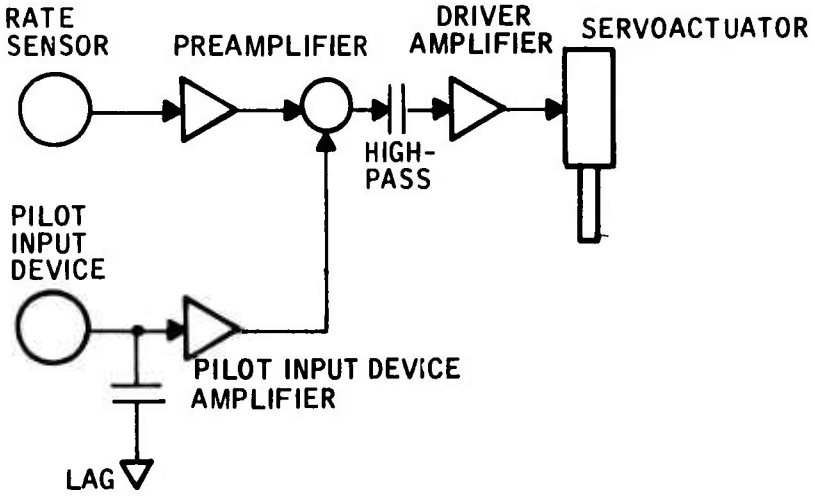

Figure 3. System Block Diagram.

Shown in Figure 4 is the complete circuit diagram of the system as originally designed for this program.

PHYSICAL CONFIGURATION

Figures 5 and 6 show the HYSAS as originally designed. It consists of a main housing which contains the high-pass capacitors, the lag capacitor, rate sensor, and pilot input device. Attached to the housing are two manifold plates which contain most of the fluid channels. Attached to these manifold plates are the amplifiers, feedback blocks and outlet block.

This complete sensor/controller mounts directly to the series servo-actuator, as shown in Figure 7. The components are described below.

Capacitors

The high-pass and lag capacitors are standard bellows closed at one end and fastened to a mounting plate by the other end.

Vortex Rate Sensor

The vortex rate sensor pickoff has been fabricated by the electroformed conductive wax process, which makes for a completely leak-free pickoff not achievable using standard machining techniques. The pickoff is unique in that the primary and secondary sinks are both incorporated into the pickoff proper (see Figure 8). This mechanization permits the use of only one exhaust plenum instead of the customary two. The difference between the customary two-sink rate sensor and this one is shown in Figure 9. It is obvious from Figure 9 that the overall size is much less with the new sensor configuration.

The null adjust vane and the built-in test vane used on past vortex rate sensors were made up of two separate mechanisms (see Figure 9a). The null adjust vane is adjusted (rotated) until the vortex rate sensor's differential pressure output is zero. The built-in test vane is depressed and then rotated, causing a bias in the fluid flow that produces a predetermined signal. It is then locked at this angle and released. Each time the built-in test vane is depressed, it then produces this calibrated sensor output signal to determine if the sensor is working properly.

In the new sensor these two vanes have been combined into a single unit. The set screw is loosened and the vane rotated to null the sensor output signal. The set screw is then locked. Rotation of the vane around this set point is restricted by the limit knot (can only be turned through a predetermined angle). A spring is used to keep the limit knob against a stop.

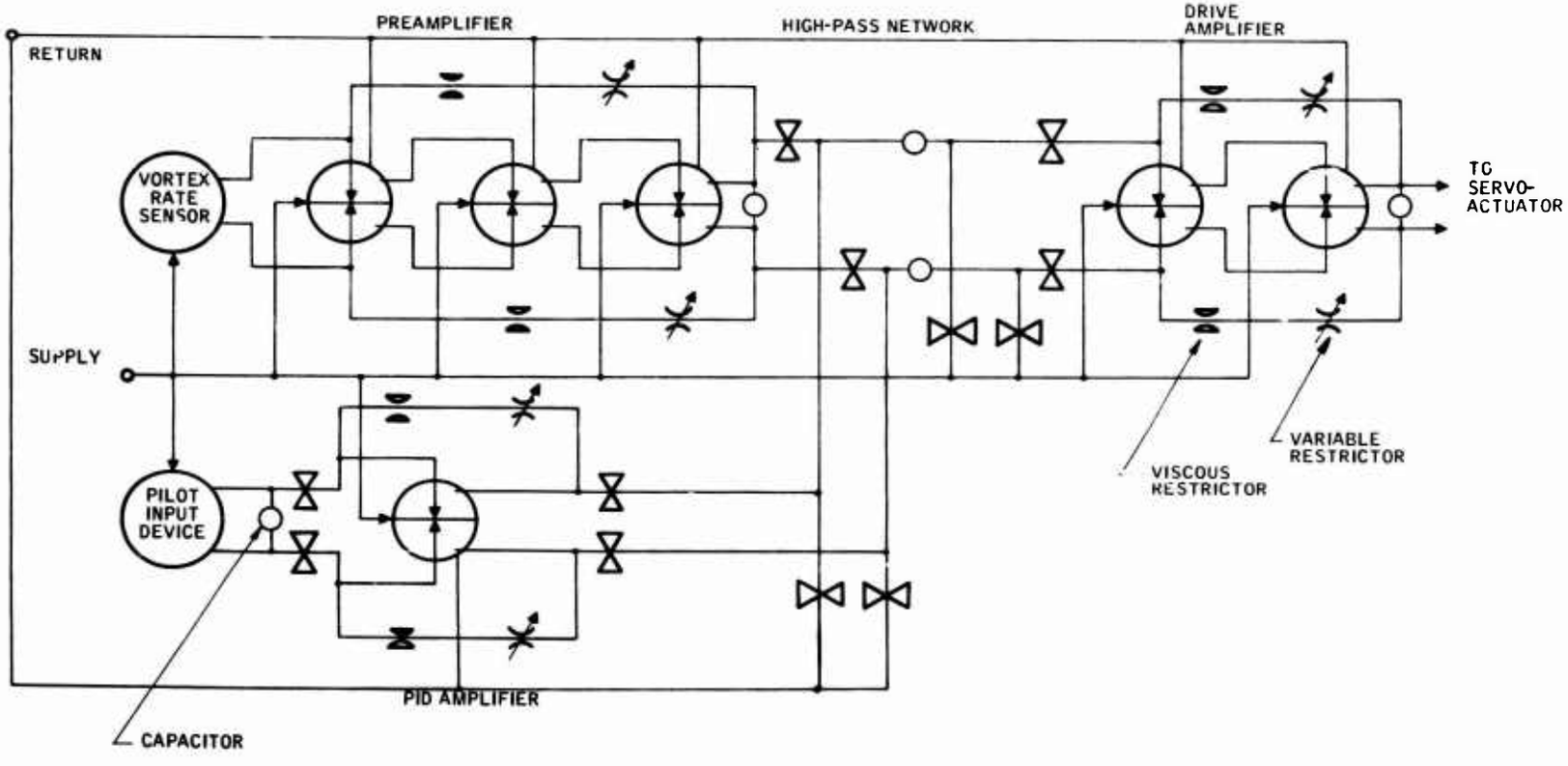

Figure 4. Circuit Diagram of Sensor/Controller.

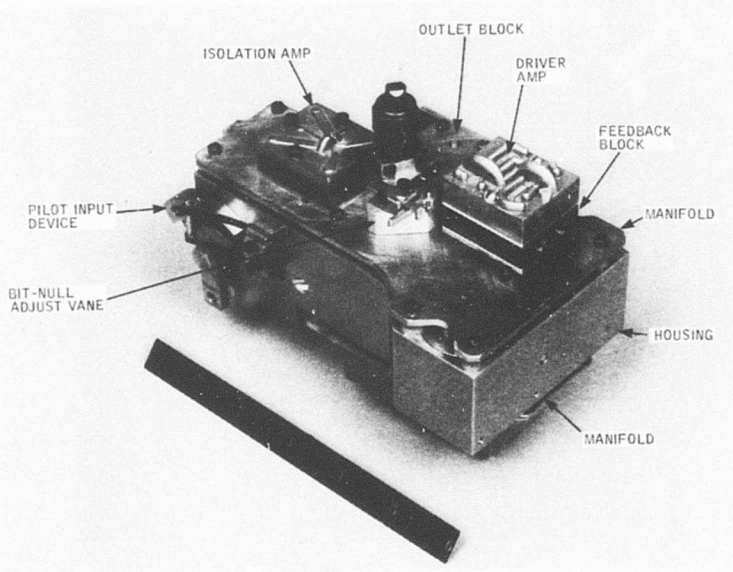

Figure 5. HYSAS - Top View.

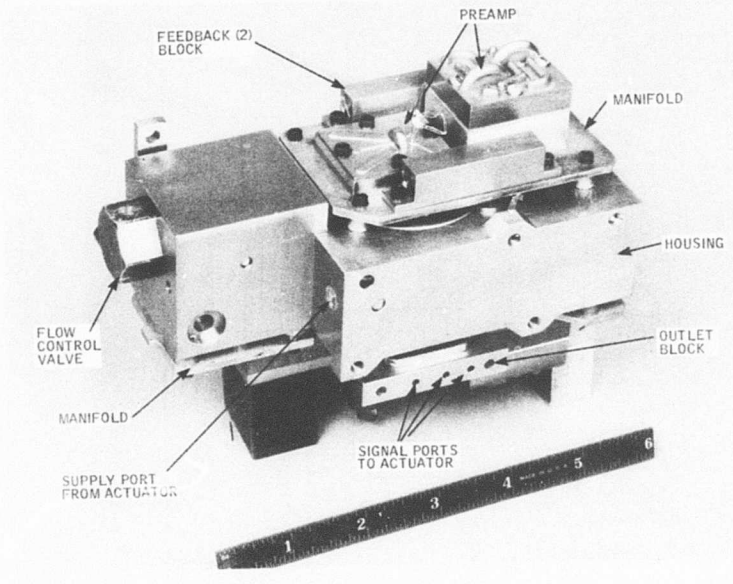

Figure 6. HYSAS - Bottom View.

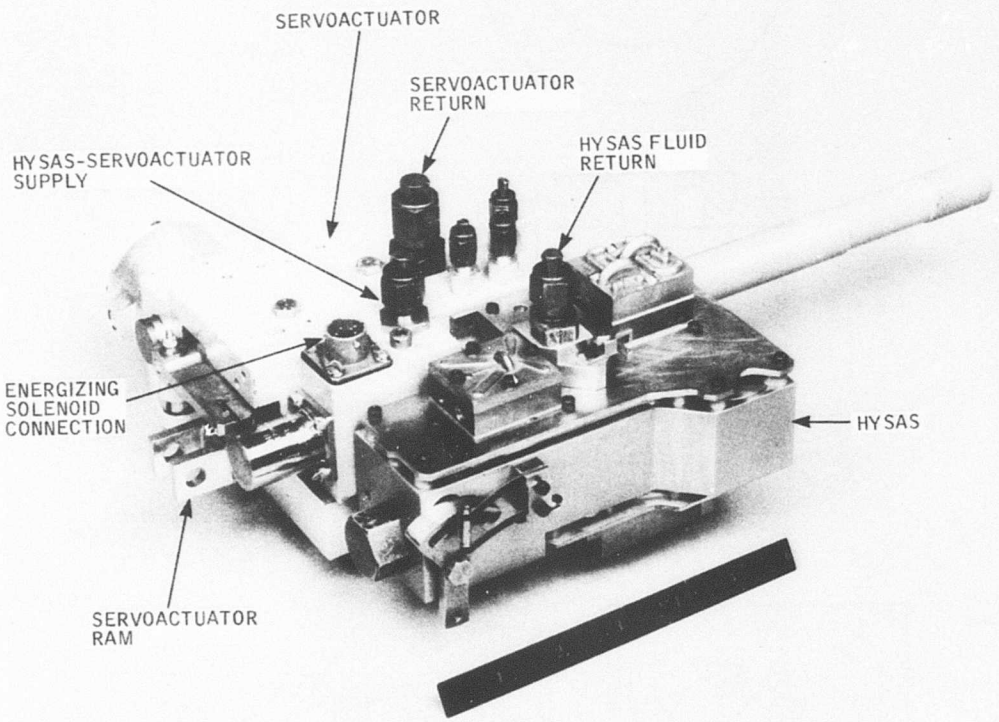

Figure 7. HYSAS Servoactuator Assembly.

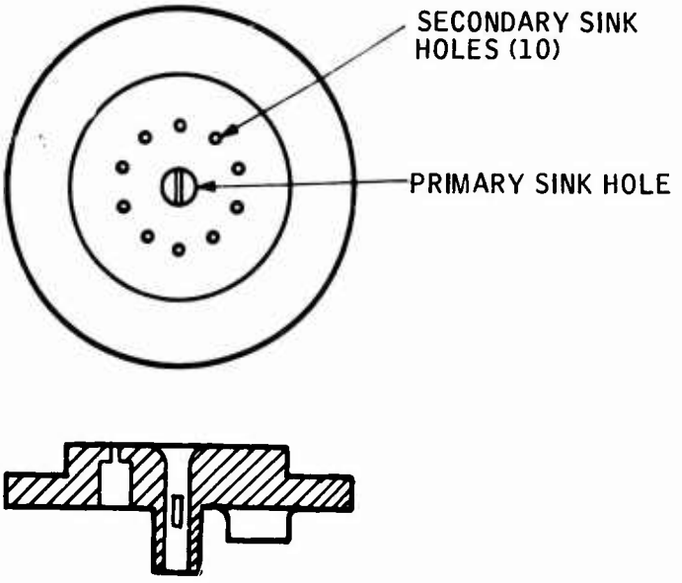

Figure 8. Rate Sensor Pickoff.

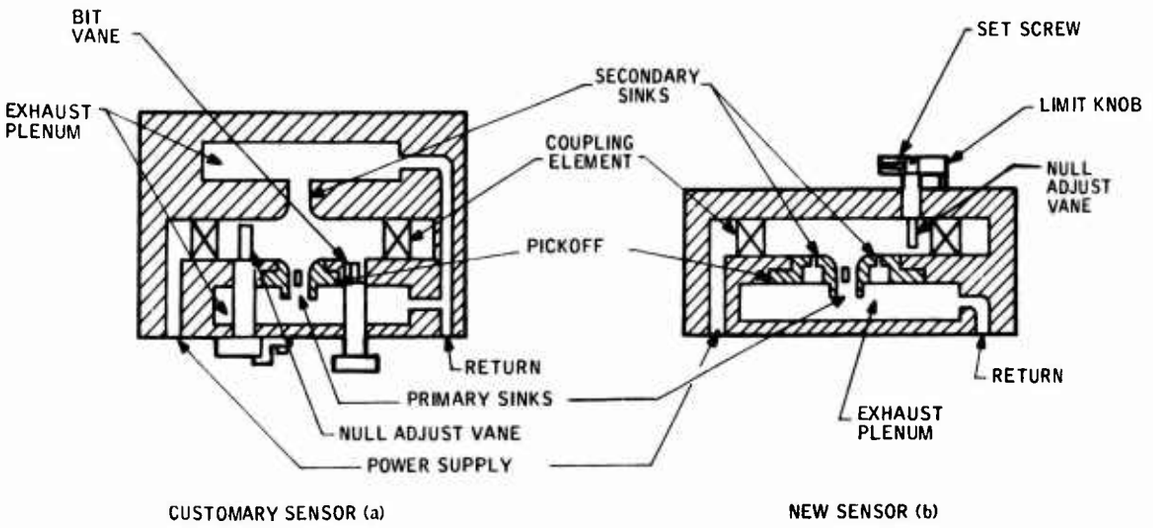

Figure 9. Rate Sensor Comparison.

Moving the knob against the spring through the preset angle produces the same BIT effect as described above. This technique reduces the hardware per sensor, reduces the number of seals, and places only one vane in the unit to affect the vortex flow (reduces noise).

Pilot Input Device (PID)

The pilot input device consists of a cam (shown in Figures 5 and 6) which operates a spool through a cam follower and shaft. This is shown schematically in Figure 10.

Fluid enters through the supply port, and passes through the metering slot into the spool and out the output ports to an amplifier. As it passes through the metering slot, it splits into two paths, producing a pressure drop, as the slot is only 0.003 inch wide. The center band on the spool covers part of the slot. With the spool centered, the openings on either side of the center band are equal in area. As the spool is moved in one direction or the other, the slot length on either side of the center band varies. This acts like two variable resistors and produces a fluidic signal that is proportional to the mechanical position of the spool. The spool is connected to the pilot's directional control linkage through the cam and a push-pull cable, resulting in fluidic signals proportional to pilot commands.

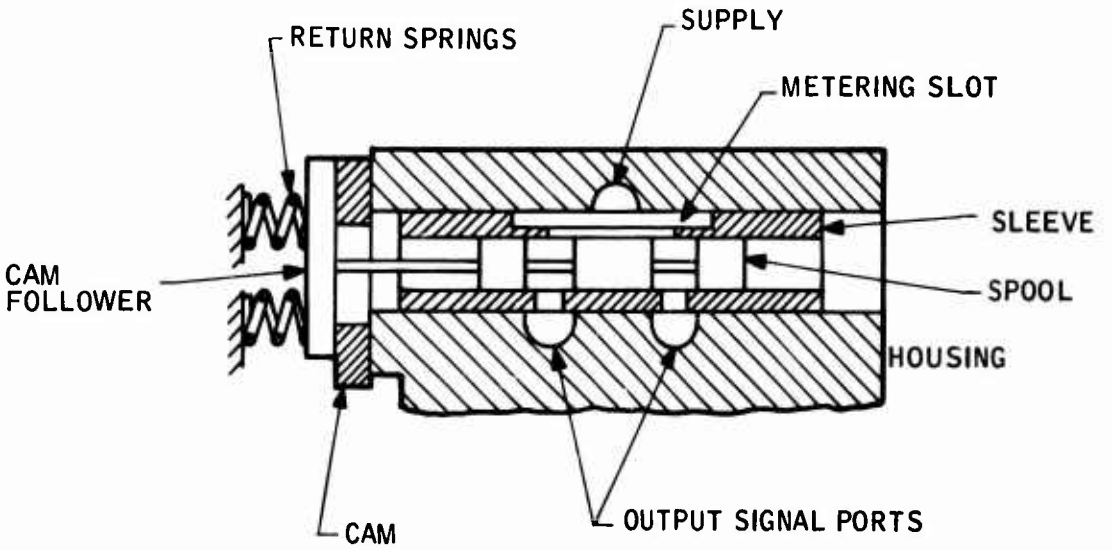

Figure 10. Pilot Input Device.

Manifolds

The manifolds consist of a stainless steel baseplate that has the channels and standoffs electroformed on one side. By electroforming the standoffs onto the baseplate, it is possible to mount components on one side of the manifold and to mount the other side to the housing, as shown in Figures 11 and 12.

The standoffs are machined after electroforming so that they are flat and will seal against the O-rings in the housing.

Amplifiers

The amplifiers are the biggest source of gain change when the temperature varies. During 1972, techniques for improving the performance of the amplifier and means of producing a constant gain versus temperature profile were investigated. The results of this effort (temperature-sensitive negative feedback) were incorporated into the design of the sensor/controller.

The technique of negative feedback is not new, but applying it to fluidics and putting a viscous resistor (hypodermic tube) in the feedback loop are new. In order to add enough feedback around a cascade to be effective, it is necessary to have high forward loop gain. To keep the package as small as possible, the normal amplifier and baseplate are manipulated so that two amplifiers are incorporated within the same plain area, port location and input-to-output phasing. The single amplifier and double amplifier are shown in Figures 13 and 14.

A 0.015-in. power nozzle single amplifier and a 0.025-in. power nozzle double amplifier were used to make up the preamp shown in Figure 3. The complete circuit is shown in Figure 15. The 180, 250, 66 and 90-lb sec/in.^{5} resistors are within the amplifier. A program has been written in the BASIC language that allows the evaluation of this circuit on the computer. By inputting the known resistances and the no-load gain of the amplifier cascade, the gain of the circuit can be computed for various Rs and Kvs. This program was used to determine the Rs and Kvs for all three cascades.

The performances of a normal amplifier circuit used in the past and the feedback circuit as shown in Figure 15 are compared in Figure 16. The improvement in performance is rather dramatic, as shown by the two curves of Figure 16. The low-temperature gain is increased and the high-temperature gain is reduced, resulting in a much flatter curve. Effort is still continuing in this area under an in-house investment program to improve the gain versus temperature capabilities, especially at low temperature conditions.

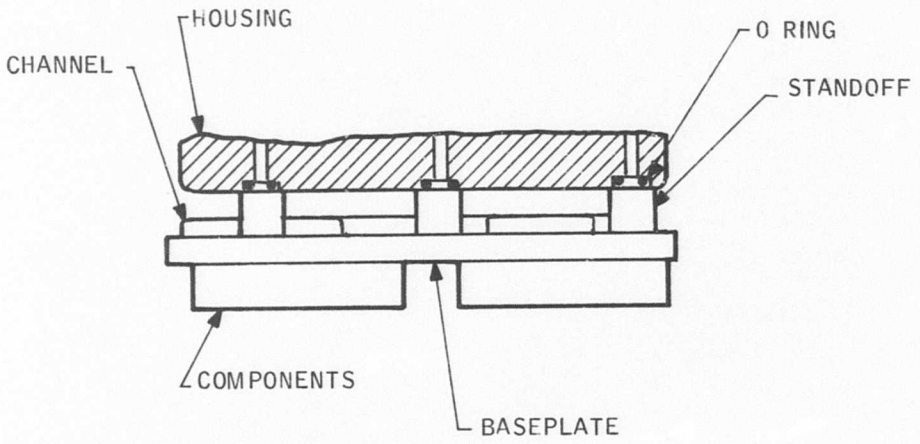

Figure 11. Manifold Cutaway.

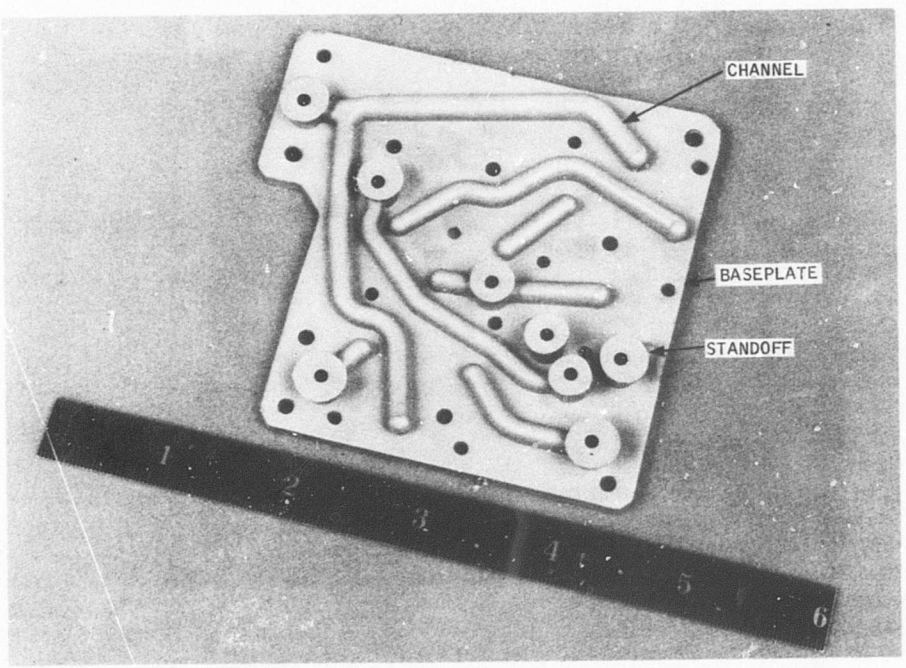

Figure 12. Manifold.

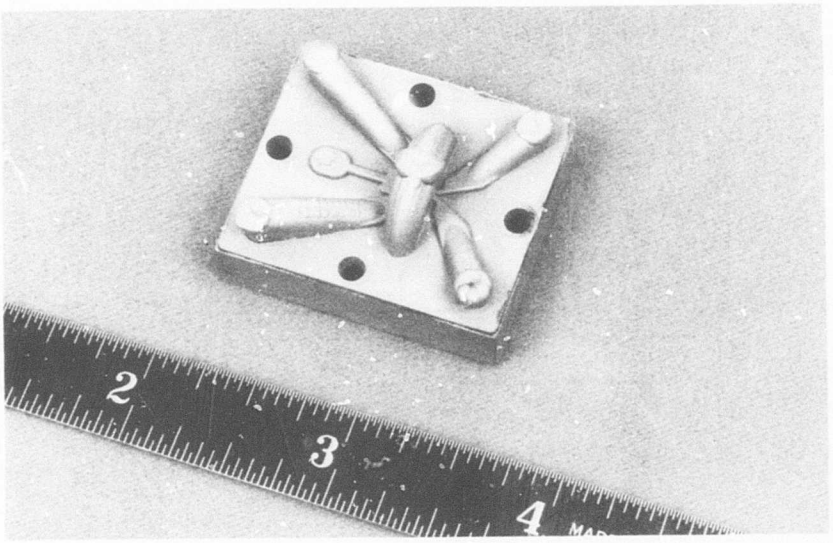

Figure 13. Single Fluidic Amplifier.

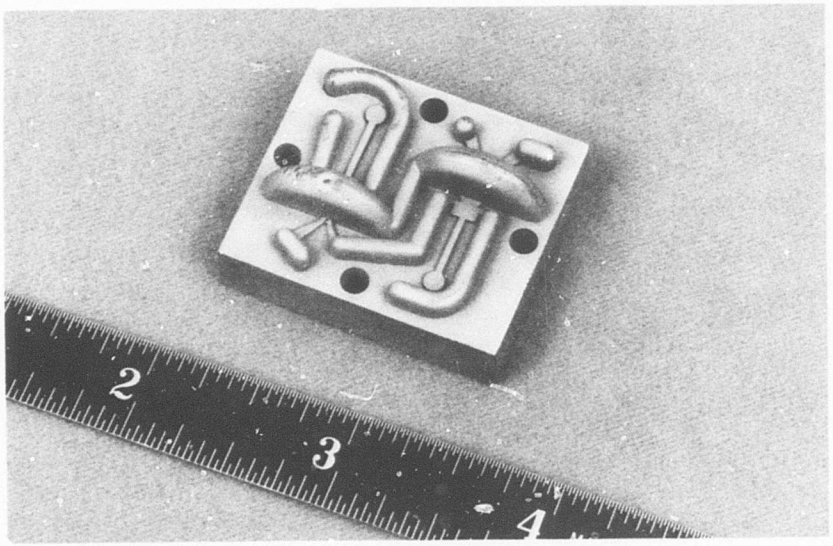

Figure 14. Double Fluidic Amplifier.

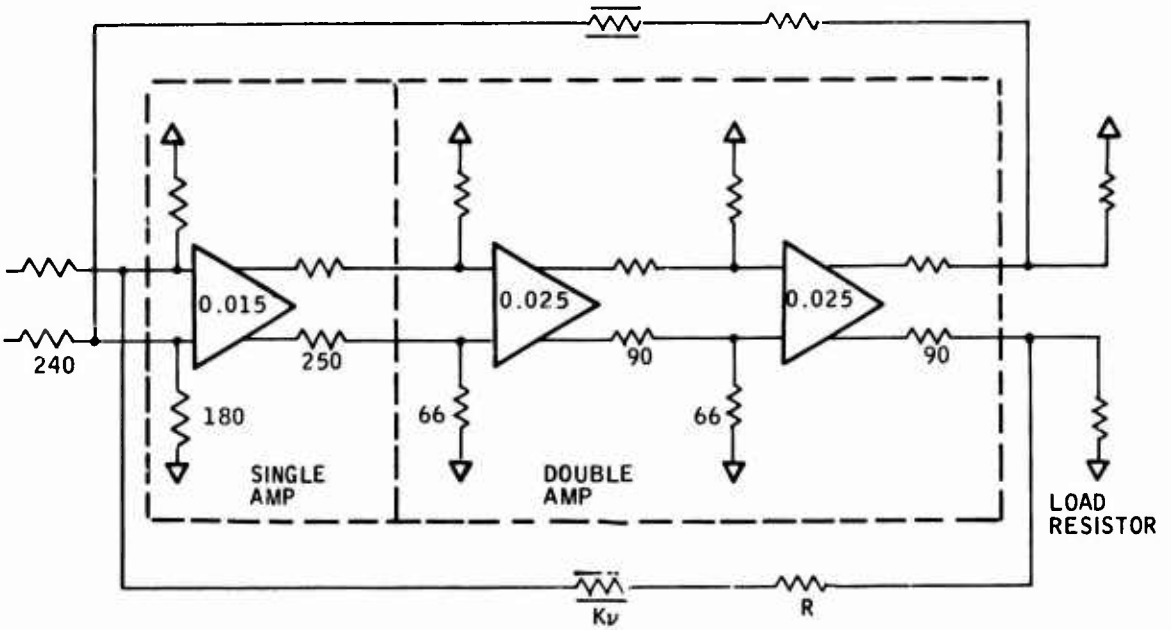

Figure 15. Amplifier Feedback Circuit.

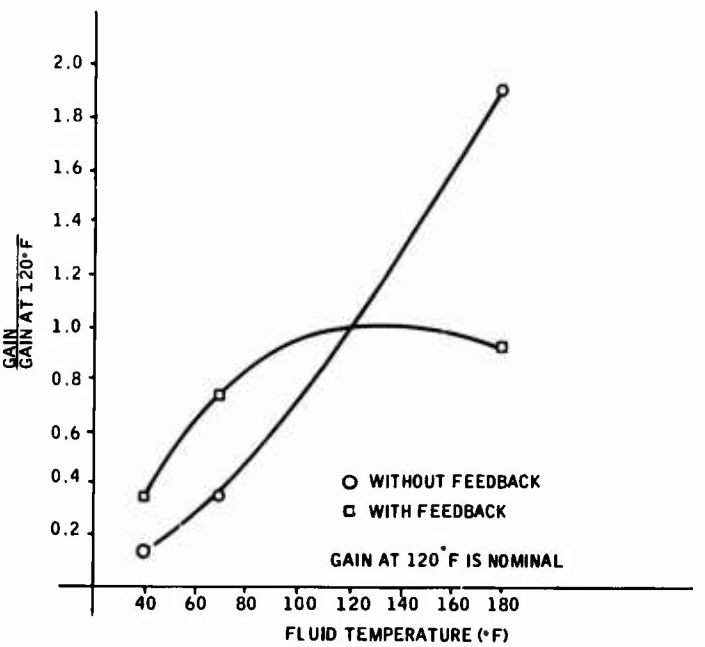

Figure 16. Amplifier Gain Versus Temperature.

MODIFICATIONS

Gain Increase

The original sensor/controller circuit shown in Figure 4 was implemented into the hardware state. At that time in the program, flight testing of an HYSAS feasibility model on board an OH-58 helicopter was being conducted under Contract DAAJ02-72-C-0111. During this flight test program, it was determined that system gain should be increased 30 percent over that determined by the analysis conducted earlier.

Circuit Change (Straight-Through Loop)

Also during the above flight test program, the aircraft exhibited an undesirable hover, out-of-ground effect (OGE) characteristic. When the pilot commanded a yaw step input with the aircraft at hover, OGE, the aircraft yaw rate of turn continued to increase to a very high level. In essence, the aircraft did not respond as a rate vehicle, but as an acceleration vehicle.

To investigate this problem, the equations of motion of the OH-58 were set up on the analog computer, and the damping derivative was changed so that the computer data agreed with the flight test data. A number of circuits were investigated, and the selected mechanization is shown in Figure 17. The additional circuit is shown by dashed lines (the analysis report is presented in Appendix I). This circuit adds a straight-through loop that bypasses the high-pass capacitors. The gain through this portion of the circuit is set at 10 percent of the high-pass loop gain. The analysis shows that this will be sufficient to make the aircraft a rate vehicle instead of an acceleration vehicle.

DEVELOPMENT TESTING

This subsection describes the calibration and testing of the sensor/controller.

Vortex Rate Sensor

The original signal pickoff used in the vortex rate sensor was fabricated by the electroformed conductive wax process. The pickoff produced a large rate sensor signal null offset. The rate sensor gain curve is shown in Figure 18. The null offset was compensated for by adding an orifice between the rate sensor pickoff and the control port of the first amplifier. Any null offset makes it difficult to calibrate the system. Pickoffs used on recent programs made with a steel blade instead of the electroformed blade have exhibited good null characteristics over the normal operating temperature range of the fluid.

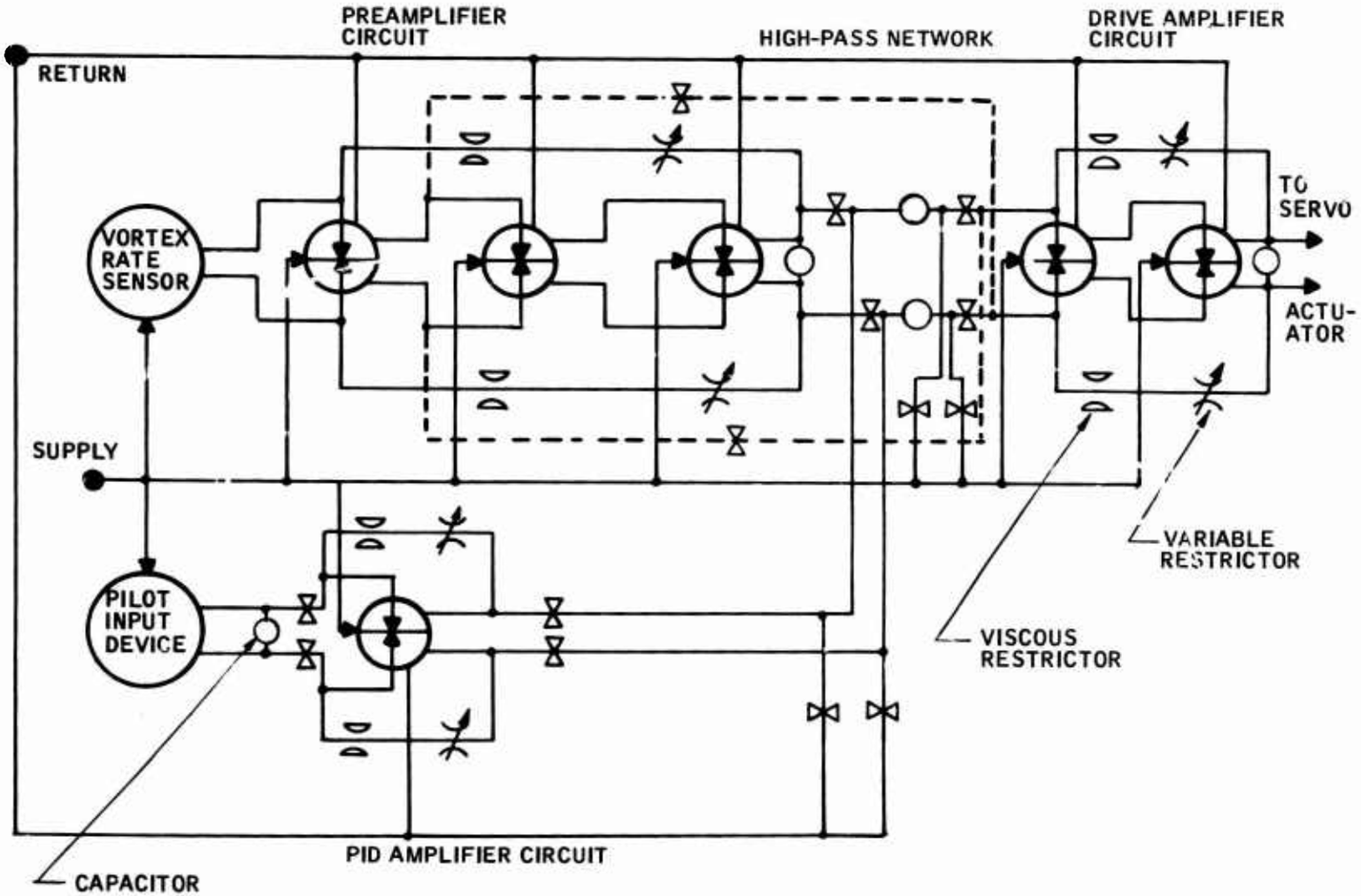

Figure 17. Circuit Diagram of Sensor/Controller With Straight-Through Loop.

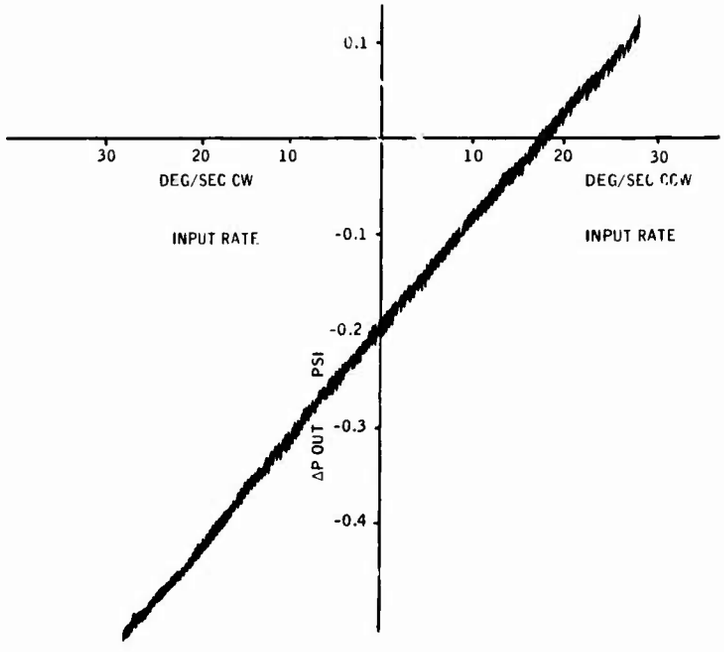

Figure 18. Vortex Rate Sensor Gain Curve.

During the program, a machined rate sensor pickoff was fabricated and tested. Rate sensor gain was about 30 percent lower than with the electroformed pickoff. Also, with the pickoff the sensor had a lower signal-to-noise ratio (so was not used).

During the temperature tests, the sensor with the electroformed pickoff exhibited a signal nonlinearity between the temperature of 116°F and 125°F. This was corrected by rounding the leading edge of the pickoff.

The vortex rate sensor generated a high noise level, 3 to 4 deg/sec; therefore, the sensor was tested dead ended, flow loaded, with orifice loads, etc., with no success. The secondary sink holes were then blocked; however, to supply the proper flow to the sensor, it was necessary to remove the flow control valve and to control the flow by another means. Under this condition the noise was only 0.5 deg/sec. The secondary sink was opened with no increase in noise. With the installation of the flow control valve, the noise increased dramatically. The flow control valve was replaced with a new unit, and the sensor noise level stayed at 0.5 deg/sec.

Amplifiers

In the original design, it was planned to correct for system null offsets by adjusting the variable feedback resistors. During testing of the sensor/controller over the temperature range, it became evident that this was not possible since the null changed with temperature. This technique would work if there were no viscous resistors in the feedback path. Balancing out the original null offset by an unbalance in the feedback path puts a different flow through one viscous resistor compared to the other. As the temperature varies, the feedback flow varies and the nonlinearity of the variable resistor (orifice law) unbalances the null, as one feedback path flow will vary more than the other. It became necessary to null each circuit open loop; then when the loop was closed, the feedback flow would be equal on both sides with no null shift.

Originally, no filter capacitors were used on the preamp circuit or driver amplifier circuit. During testing, it became obvious that they were necessary in order to prevent the circuit from oscillating. It was not necessary to add one to the PID amplifier circuit, as the feedback gain was not sufficient to cause it to oscillate.

Circuit Change (Relocation of Straight-Through Loop Connection)

During the calibration of the system, particularly the straight-through loop, the circuit oscillated when the straight-through loop gain was set at 10 percent of the high-pass loop gain. Closer examination of the circuit indicated the circuit could be looked at as a positive feedback circuit with a high pass in the forward loop. This arrangement would cause the circuit to oscillate at a frequency governed by the capacitor time constant. This was corrected by reducing the forward loop gain and decreasing the feedback gain. The straight-through loop was connected one stage toward the high-pass capacitor. Figure 19 shows the final circuit. The simple relocation of the straight-through loop connection accomplished both correcting changes. With only one amplifier in the forward loop, its gain was reduced. Also, by increasing the amplifiers in the total straight-through loop circuit, it was necessary to increase the resistance to get the proper gain, thus reducing the positive feedback gain.

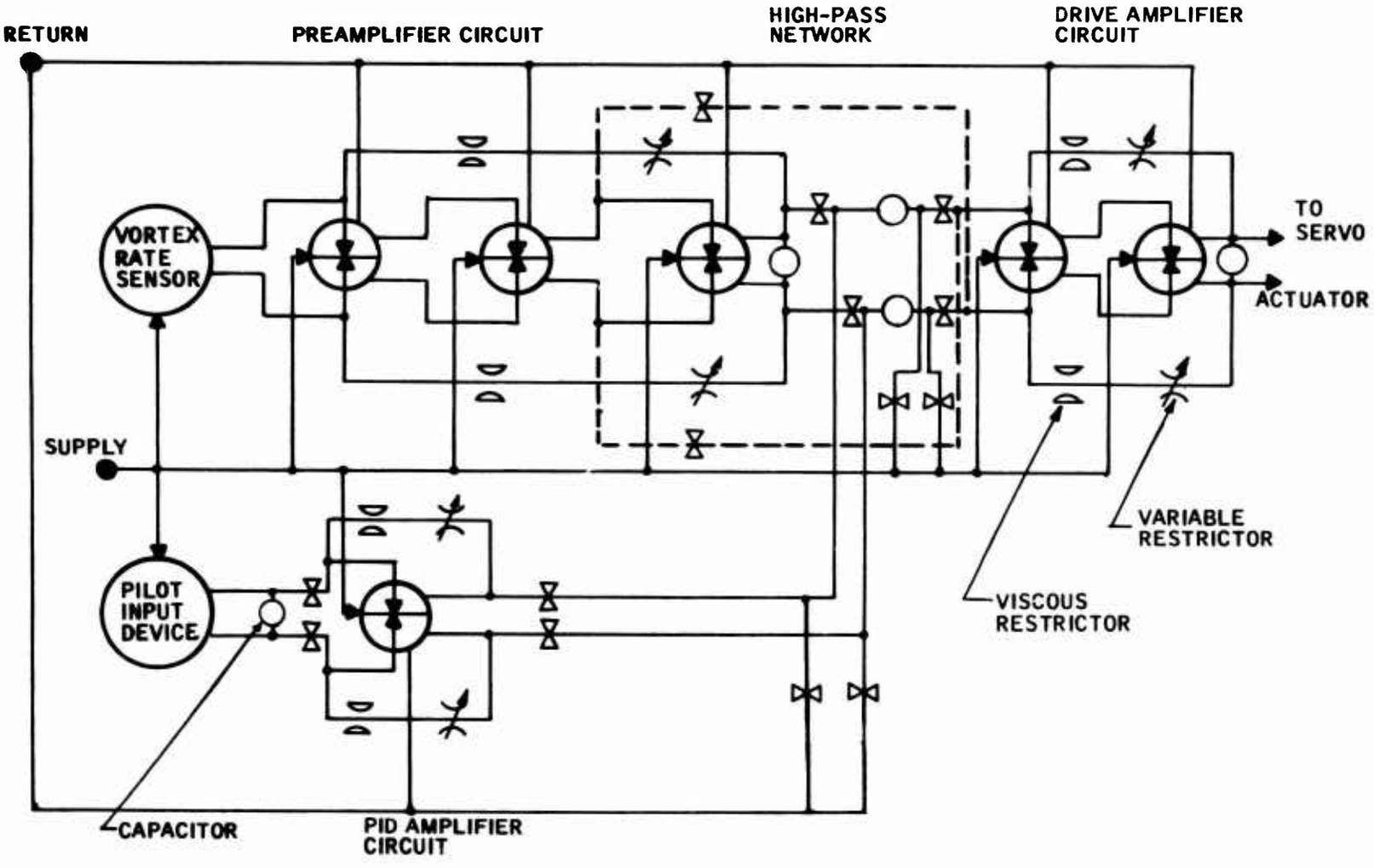

Figure 19. Final Sensor/Controller Circuit Diagram.

SECTION III

ACCEPTANCE TESTS

The YG1116A01 Hydrofluidic Yaw Axis Stability Augmentation System was subjected to the tests specified in the test plan, Appendix II. The detail specification is contained in Appendix III.

The test data is presented in Figures 20 and 21 at 70°F, Figures 22 and 23 at 90°F, Figures 24 and 25 at 120°F, and Figures 26 and 27 at 180°F. Table I summarizes the system performance.

The sensor/controller and servoactuator were vibrated as specified in the test plan. During the vibration testing, no adverse effects were encountered.

Part way through the after-vibration tests the servoactuator ceased to operate. It would not move when an input signal was applied and would not center and lock when the fluid supply solenoid valve was deenergized. The unit was returned to the manufacturer for repair. The nozzles of the servoactuator first stage had become contaminated. After cleaning and assembly, the unit would not meet the frequency response requirements, thereby delaying delivery.

Because of the delay in receiving the servoactuator and to prevent additional delay in this program, an adapter was made so that the sensor/controller could be mounted on the servoactuator that was used with the YG1105A01 sensor/controller.

TABLE I. SYSTEM PERFORMANCE

	Initial					After Vibration*
	40°F	70°F	90°F	120°F	180°F	120°F
Rate Loop Gain (in./deg/sec)	**	0.00705	0.0218	0.03	0.0175	0.028
PID Loop Gain (in./in.)	**	6.5	6.5	6.5	6.5	2.0 ***
Noise (in.)	0	0.025	0.028	0.0395	0.0395	0.042
Null (in.)	**	0.103	0.085	0.0226	0.0175	0

* This performance is with the YG1105A01 servoactuator.

** Not readable due to very low gain.

*** Actuator change after vibration resulted in circuit change which reduced PID gain. This will be evaluated during flight test.

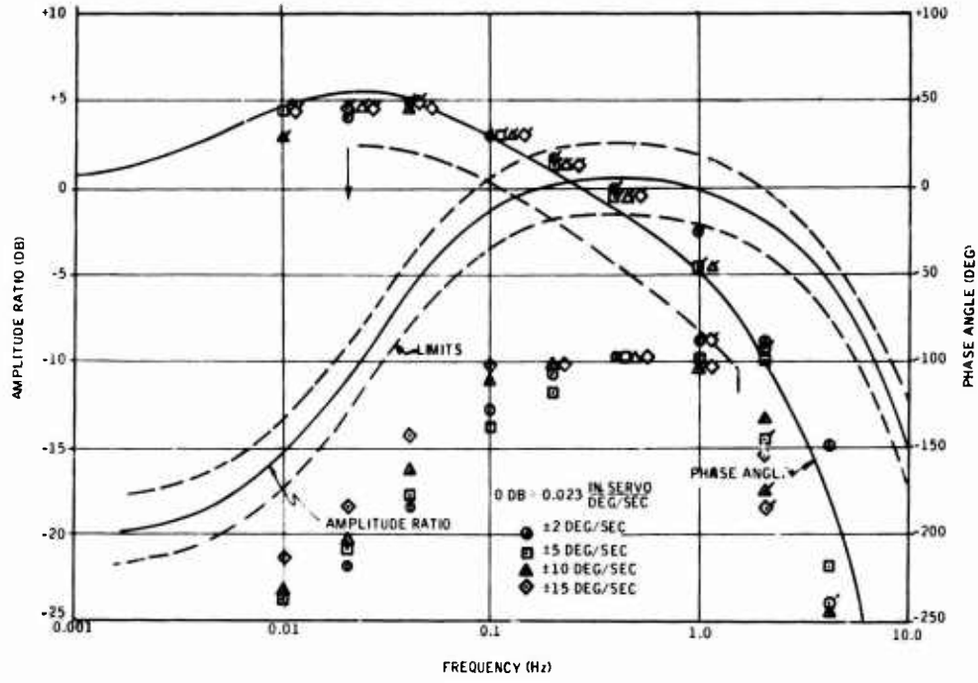

Figure 20. Rate Transfer Function - 70°F.

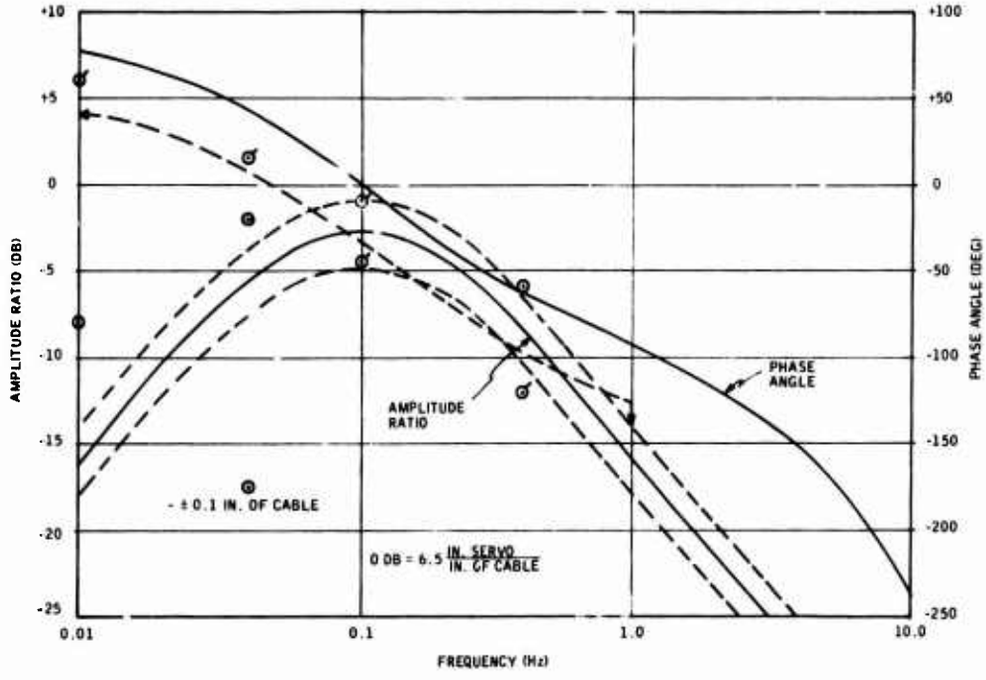

Figure 21. Pilot Input Transducer Transfer Function - 70°F.

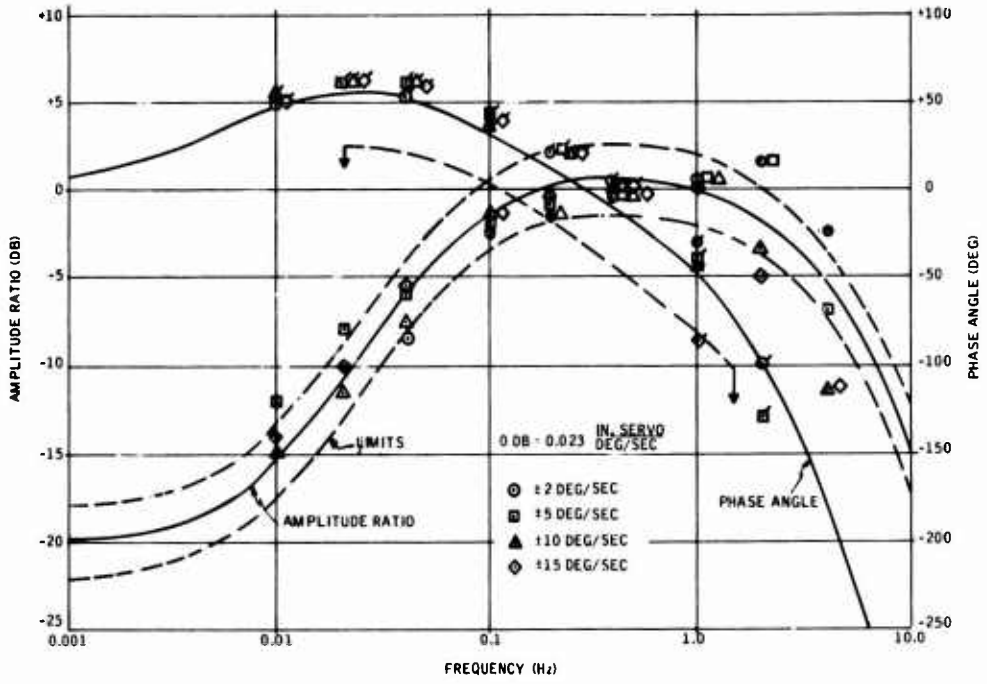

Figure 22. Rate Transfer Function - 90°F.

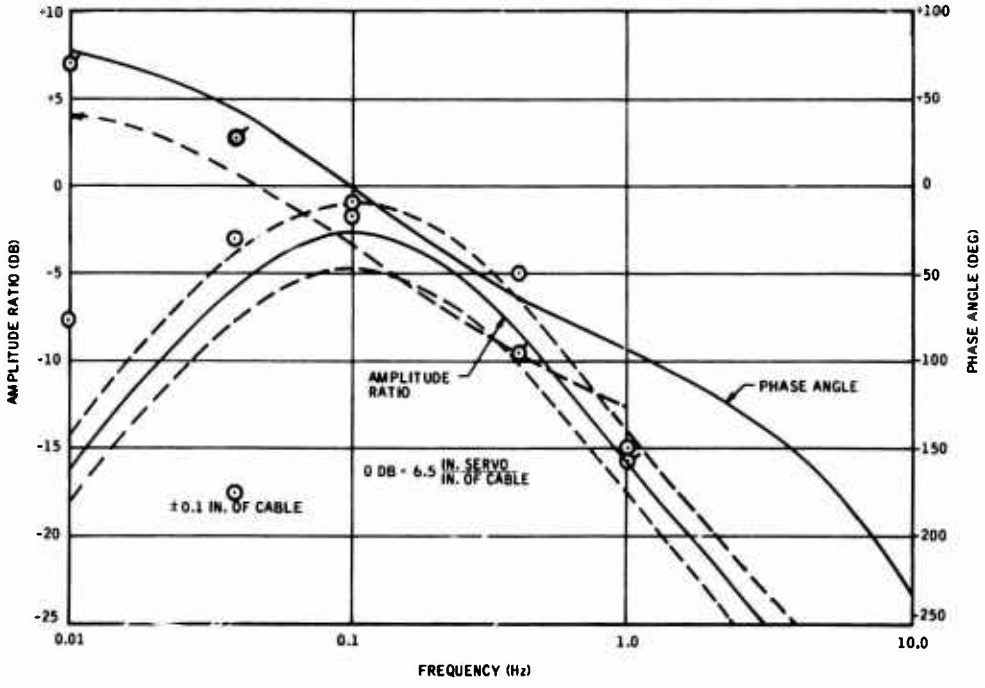

Figure 23. Pilot Input Transducer Transfer Function - 90°F.

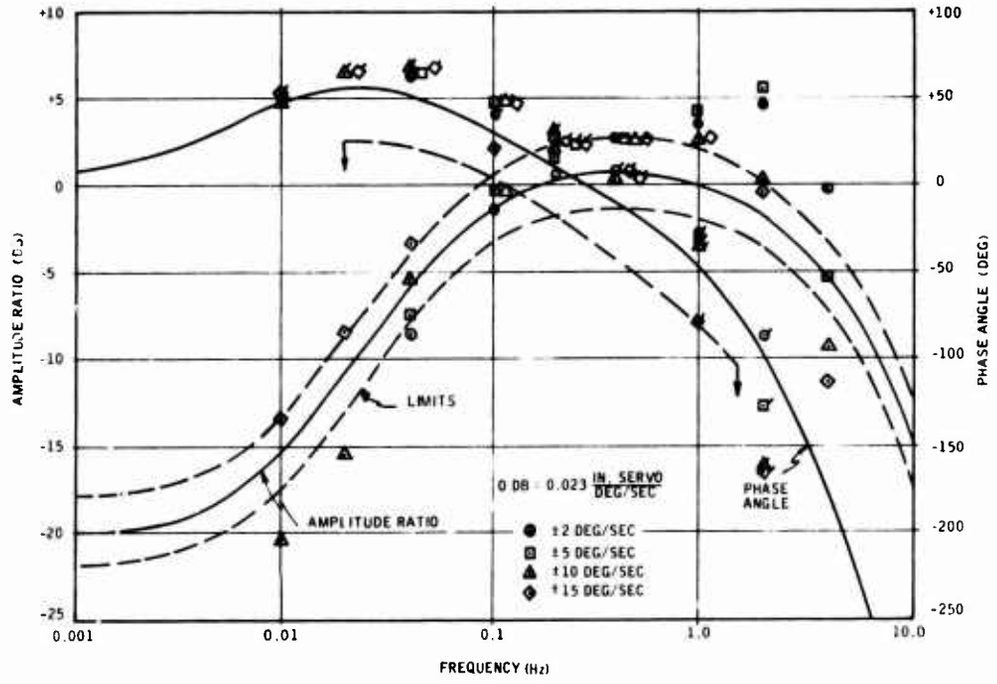

Figure 24. Rate Transfer Function - 120°F.

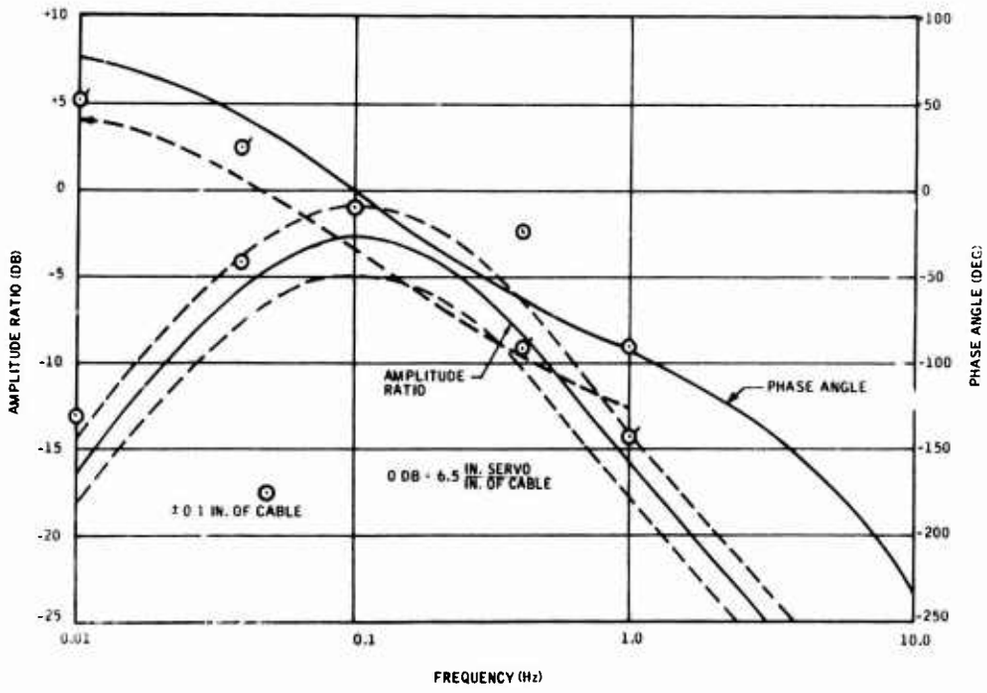

Figure 25. Pilot Input Transducer Transfer Function - 120°F.

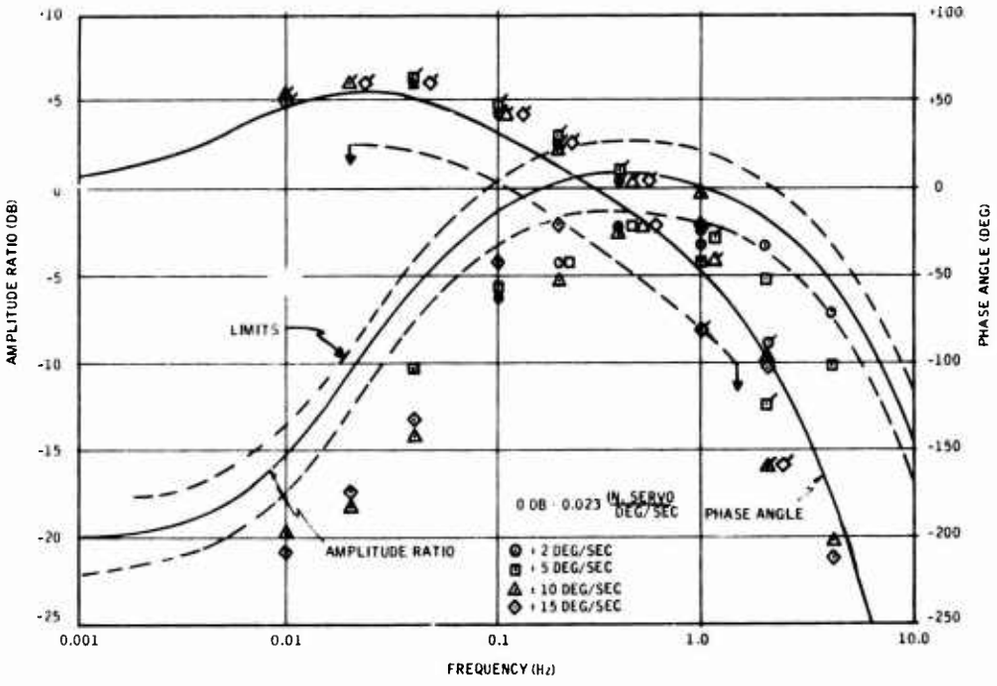

Figure 26. Rate Transfer Function - 180°F.

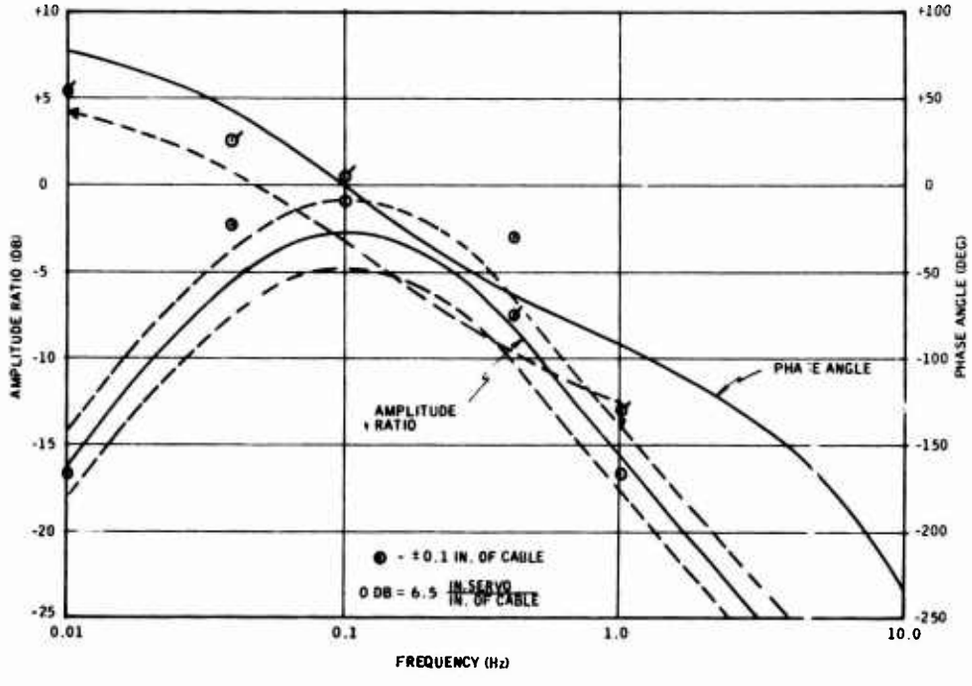

Figure 27. Pilot Input Transducer Transfer Function - 180°F.

It was necessary to modify the YG1116A01 sensor/controller because of a slight difference in the gains of the two servoactuators. Also, the servoactuator was of a type that when driven by a hydrofluidic amplifier it exhibits underdamped frequency response characteristics (peaking). This peaking, in conjunction with the negative feedback on the drive amplifier generated excessive noise. The reasoning behind this can best be explained as follows. The peaking of the servoactuator output shaft shows up at the signal ports to the servoactuator. Using the circuit of Figure 19 any input at the drive amplifier circuit, - servoactuator interface will be fed back to the input to the drive amplifier. Assume a step input is generated into the drive amplifier circuit, this in turn feeds a signal into the servoactuator. The servoactuator moves, overshoots due to the underdamped characteristic, and in returning to the commanded position feeds a signal into the output of the drive amplifier circuit. This signal in turn passes through the feedback loop to the input to the drive amplifier. This produces another input signal and the process is repeated. This was eliminated by replacing the double amplifier with a single amplifier and eliminating the negative feedback loop in the drive amplifier circuit. The high gain of the drive amplifier was not needed when the negative feedback was removed.

The sensor/controller and servoactuator were tested, and the results are shown in Figures 28 and 29.

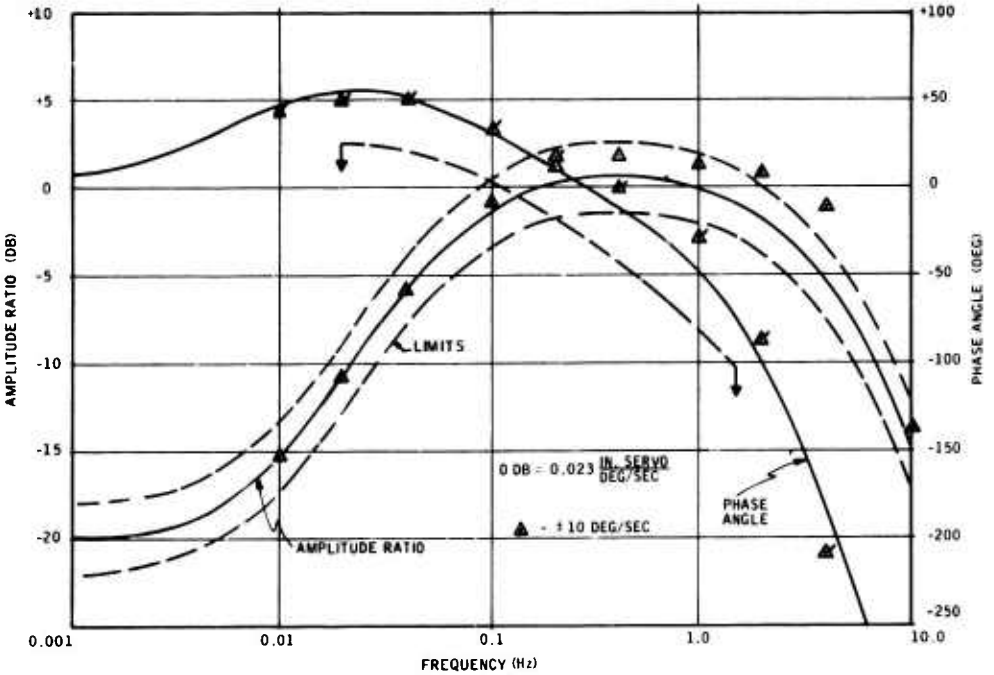

Figure 28. Rate Transfer Function - 120°F (After Vibration).

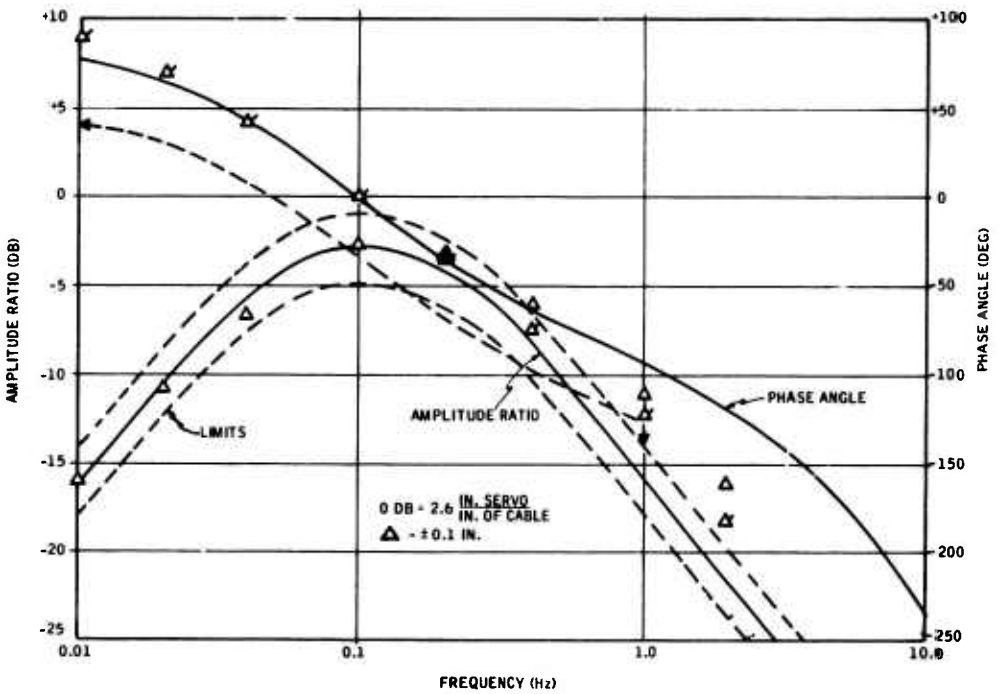

Figure 29. Pilot Input Transducer Transfer Function - 120°F (After Vibration).

SECTION IV
CONCLUSIONS AND RECOMMENDATIONS

CONCLUSIONS

- The system performance can be improved with the addition of negative feedback around the various amplifier circuits. It is not a complete solution to the low-temperature problem, but greatly improved the system performance.
- The BIT mechanism and null adjust mechanism could be successfully combined into a single unit. This reduces the number of parts, eliminates a hydraulic seal to ambient, and reduces to one the obstructions in the vortex chamber of the vortex rate sensor.
- Two amplifiers can be combined into an area normally required for one amplifier. The double amplifier phasing and hole pattern was the same as a single amplifier; thus, they are directly interchangeable.
- The manifold can be made with standoffs for mounting and also with O-ring seal surfaces on one side. This allows components to be mounted on both sides of the manifold.
- To obtain proper system functioning, a straight-rate loop is required around the high-pass capacitors with the junction point inside the closed-loop preamp circuit.
- The system has been subjected to all the flightworthiness tests and is ready for flight test.

RECOMMENDATION

- Each amplifier circuit with viscous-type negative feedback must be nulled open-loop so temperature effects do not cause null shifts. For ease of calibration a means of nulling each circuit in the open loop condition should be incorporated into future systems that use viscous restrictors in the feedback loop.

APPENDIX I

OH-58A HYDROFLUIDIC YAW SAS ANALYSIS RESULTS

SUMMARY

At hover, the OH-58A helicopter has an undesirable characteristic of developing an excessively high yaw rate for a small step pedal input. As shown in Figure 30, a pedal input of about 0.35 inch causes a yaw rate in excess of 55 deg/sec for the free vehicle. The YG1105A01 yaw SAS does not alleviate this problem, since yaw rate feedback is high-passed so that the ultimate rate is undiminished. Several proposed fixes for this problem were evaluated using an analog computer simulation. Of these fixes, one using straight-through yaw rate at a gain of about 10 percent that of the high-passed yaw rate appeared to be the most satisfactory, from the standpoint of ease of implementation and of effectiveness in correcting the problem without degrading the existing turn coordination.

DISCUSSION

The first step taken to solve the OH-58A hover problem was to repatch the analog simulation used in the original analysis. The analog diagram and pot settings used are reproduced in Figure 31 and Table II for completeness. After the results were duplicated, indicating satisfactory computer operation, aerodynamic coefficients were varied to simulate flight test results (Figure 30). The variation of the yaw rate damping derivative, N_r, from the nominal value of 520 to 350 produced results similar to flight test. This can be seen in Figure 32, where the free aircraft was subjected to a 0.35-in. pedal step. The resulting yaw rate trace agrees quite closely with the flight test results in Figure 30. In Figure 32b, a 0.55-in. pedal step was used to force the aircraft with the yaw damper engaged, and the resulting yaw rate trace agrees with similar traces from flight test. This tends to give credibility to the analog model used, with $N_r = 350$.

Each of the systems shown in Figure 33 was investigated at hover to determine how effectively the yaw rate problem was dealt with, and at 120 kn for turn coordination deterioration. Figures 34 and 35 show the responses of each of the above systems for a 0.35-in. pedal step input, with the yaw damping derivative $N_r = 350$. The free aircraft response is seen first, and again the high yaw rate developed is evident. The nominal SAS is seen to slow the rate of divergence somewhat, but yaw rate still builds to an excessive level quickly. Next, a 10-sec rather than a 2-sec high pass is used (System 2). This system

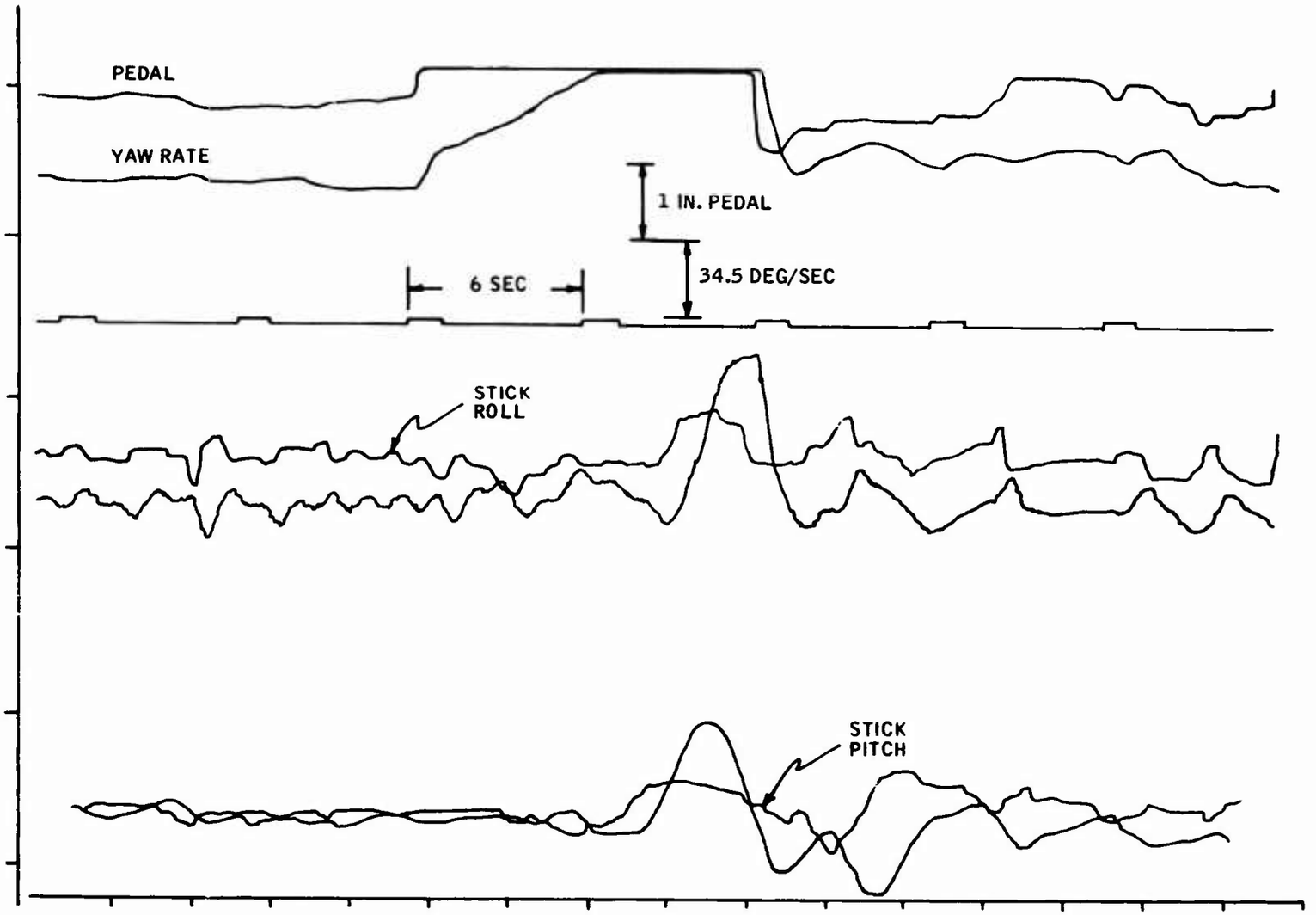

Figure 30. OH-58A Pedal Response.

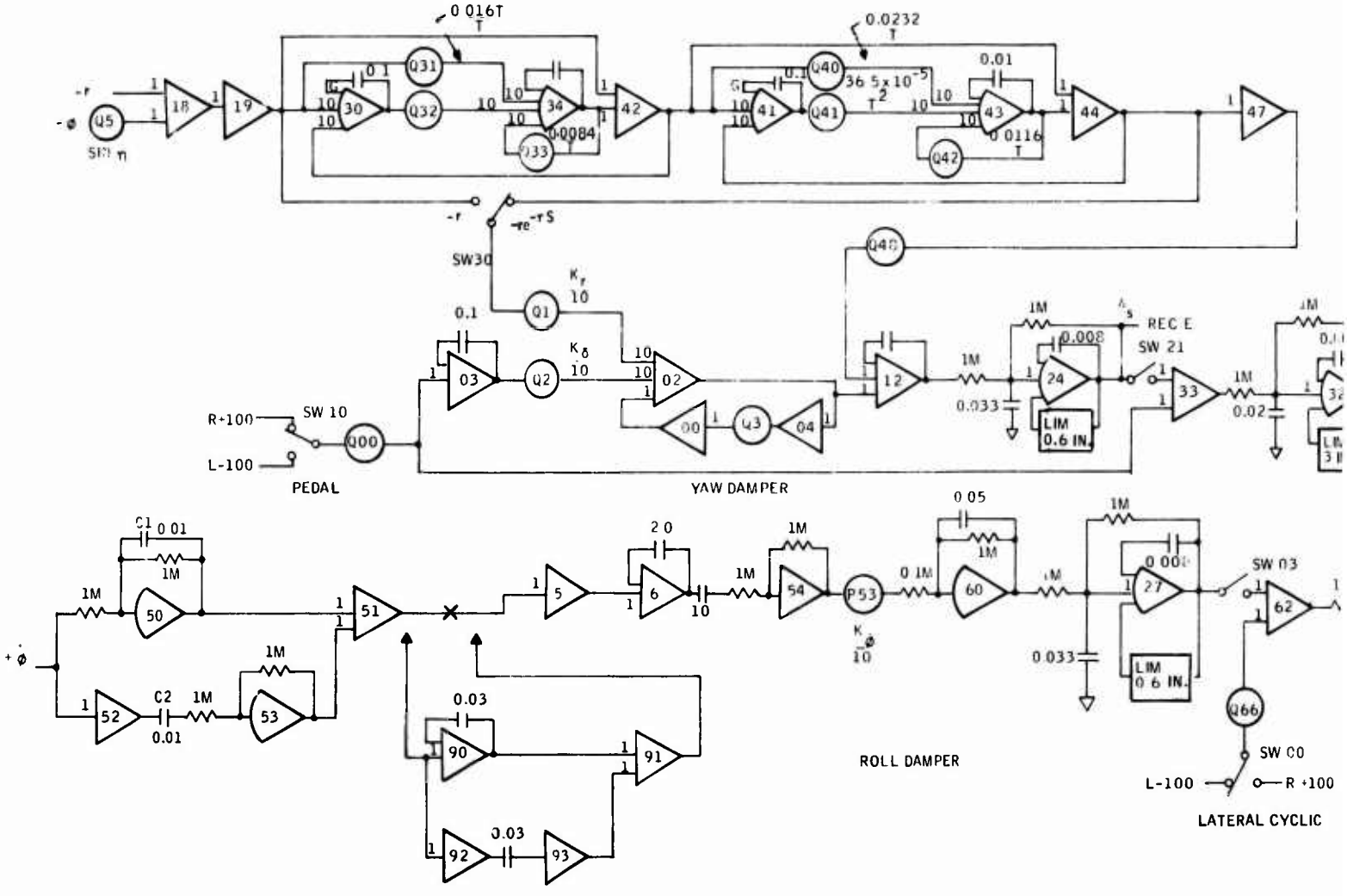

(TO EVALUATE SENSOR WITH $e^{-0.06S}$ CHARACTERISTIC ADD THIS CIRCUIT AT POINT "X". ALSO, CHANGE C1 AND C2 FROM 0.01 μf TO 0.03 μf

Figure 31. OH-58A Analog Simulation.

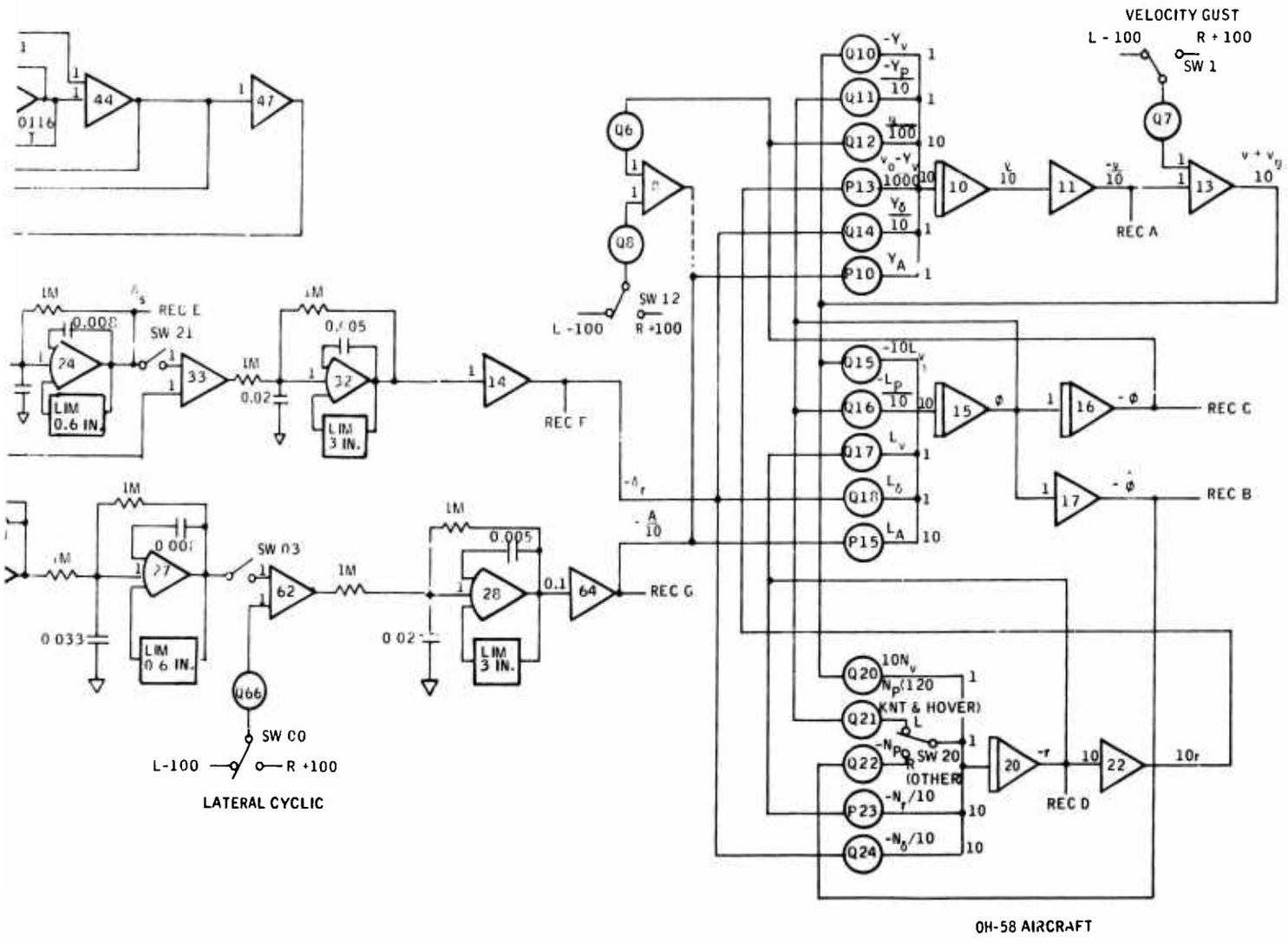
VELOCITY GUST
L - 100
R + 100
SW 1
Q7
Q10
Q11
Q12
P13
Q14
P10
Q6
Q8
SW 12
L -100
R +100
REC A
REC E
SW 21
REC F
REC G
SW 03
SW C0
L-100
R +100
LATERAL CYCLIC
Q15
Q16
Q17
Q18
P15
REC C
REC B
Q20
Q21
Q22
P23
Q24
SW 20
(OTHER
KNT & HOVER)
REC D
OH-58 AIRCRAFT

TABLE II. OH-58A ANALOG SIMULATION POTENTIOMETER SETTINGS

Parameter	Potentiometer	Aerospace Data, K_n Hover	20	40	60	80	100	120
$-Y_v$	Q10	038	058	096	135	170	208	250
$-Y_p/10$	Q11	180	224	260	260	265	236	212
$g/100$	Q12	322	322	322	322	322	322	322
$U_o-Y_r/1000$	P13	012	033	066	100	133	168	201
$Y_\delta/10$	Q14	118	105	098	110	145	167	192
$-10\ L_v$	Q15	250	280	360	500	610	720	860
$-L_p/10$	Q16	163	195	226	237	230	203	174
$+L_r$	Q17	220	320	470	640	670	900	1000
$+L_\delta$	Q18	590	530	490	590	730	850	960
$+10\ N_v$	Q20	210	195	330	450	560	660	750
$+N_p$	Q21	035	SW 20 Left for Hover and 120					042
$-N_p$	Q22	SW 20 RT	320	390	310	17	035	SW 20 RT
$-N_r/10$	P23	035 052	075	110	154	186	218	260
$-N_\delta/10$	Q24	140	122	116	139	172	198	230
$+Y_A$	P10	800	800	800	800	810	850	910
$+L_A$	P15	740	740	750	740	760	800	840

Parameter	Potentiometer	Time Delay, sec 0.050	0.030	0.075	0.100	0.060
$0.0168/T$	Q31	0.335	0.560	0.225	0.168	0.2800
$0.00046/T^2$	Q32	0.184	0.510	0.082	0.046	0.1275
$0.0084/T$	Q33	0.168	0.280	0.112	0.084	0.1400
$0.0232/T$	Q40	0.463	0.775	0.310	0.232	0.3870
$0.000365/T^2$	Q41	0.146	0.406	0.065	0.036	0.1012
$0.0116/T$	Q42	0.232	0.387	0.155	0.116	0.1935

SW 30 Left for Zero Time Delay-Right for Other

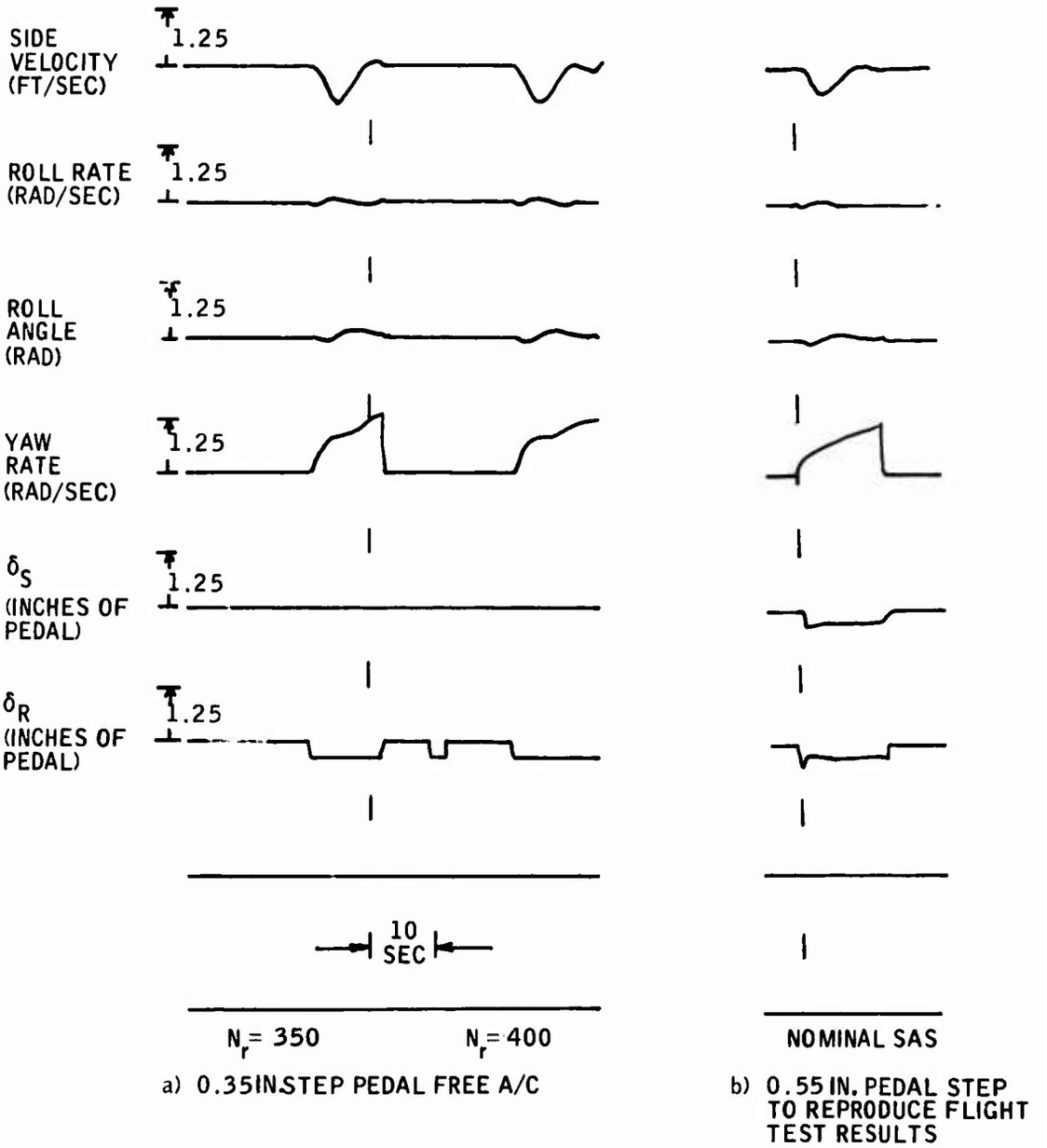

Figure 32. Duplication of Flight Test Results.

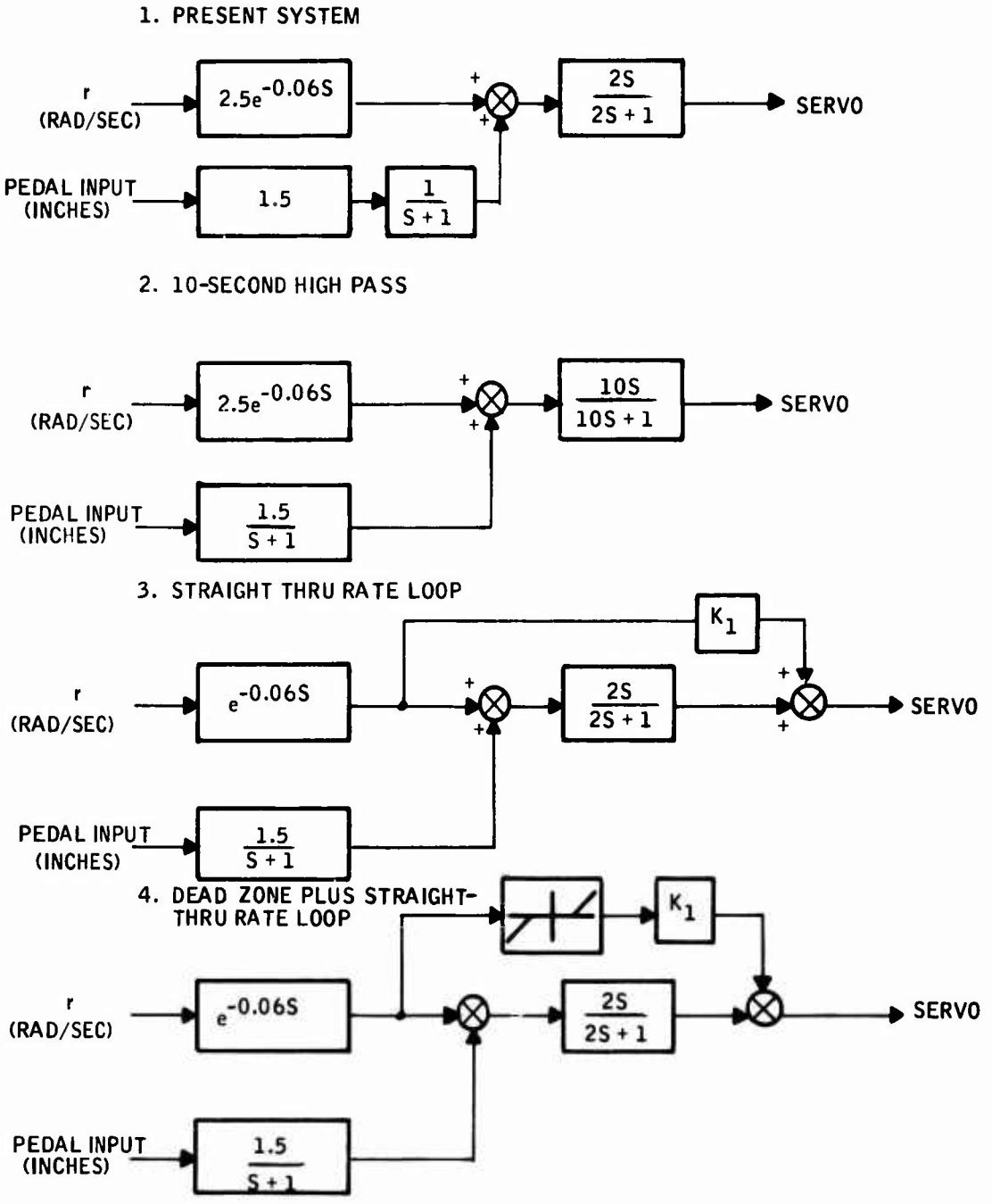

Figure 33. Circuits To Solve Rate Buildup Problem.

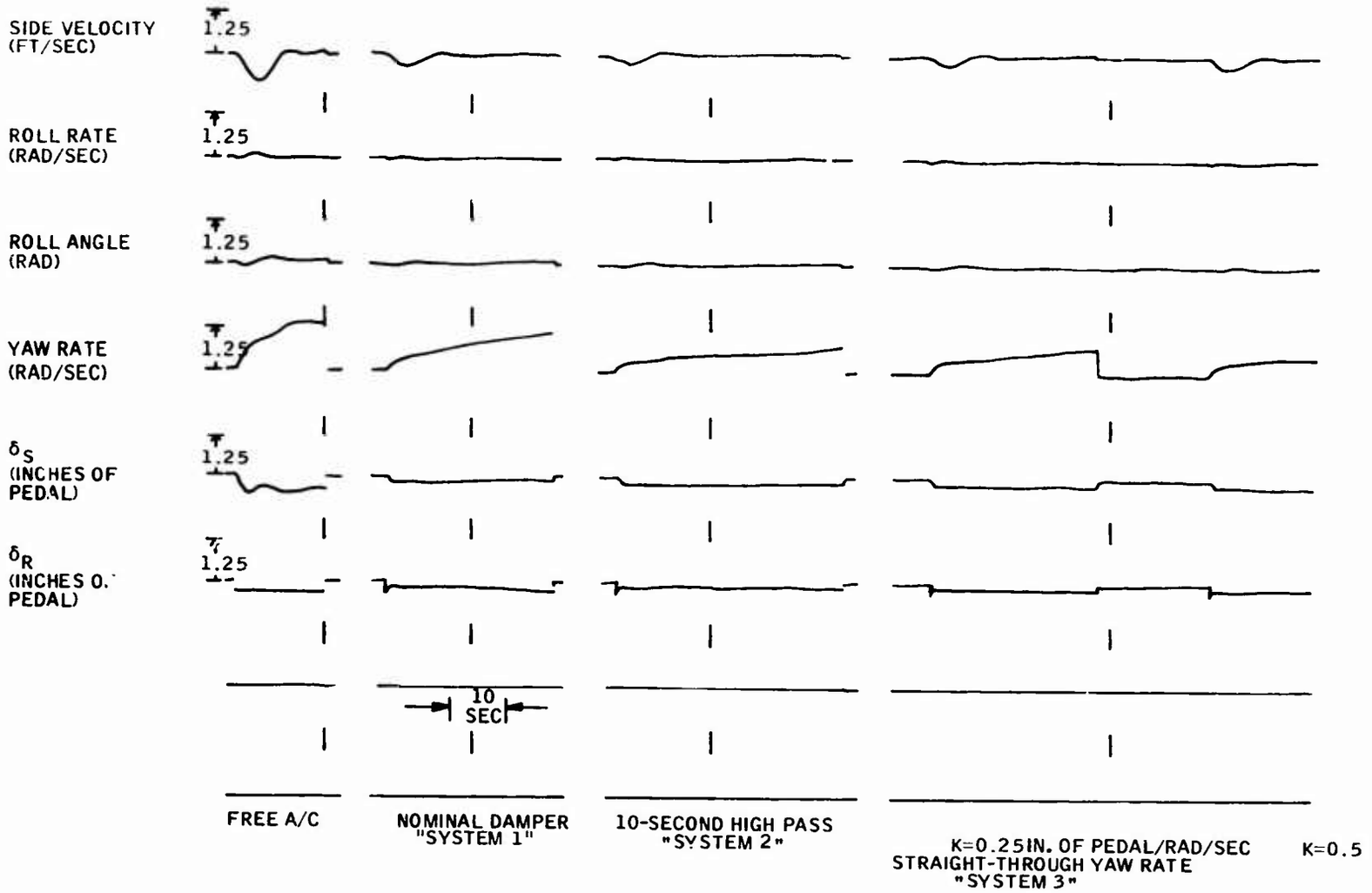

Figure 34. Responses for 0.35-In. Pedal Steps With Proposed Fixes - N_r = 350 (Hover).

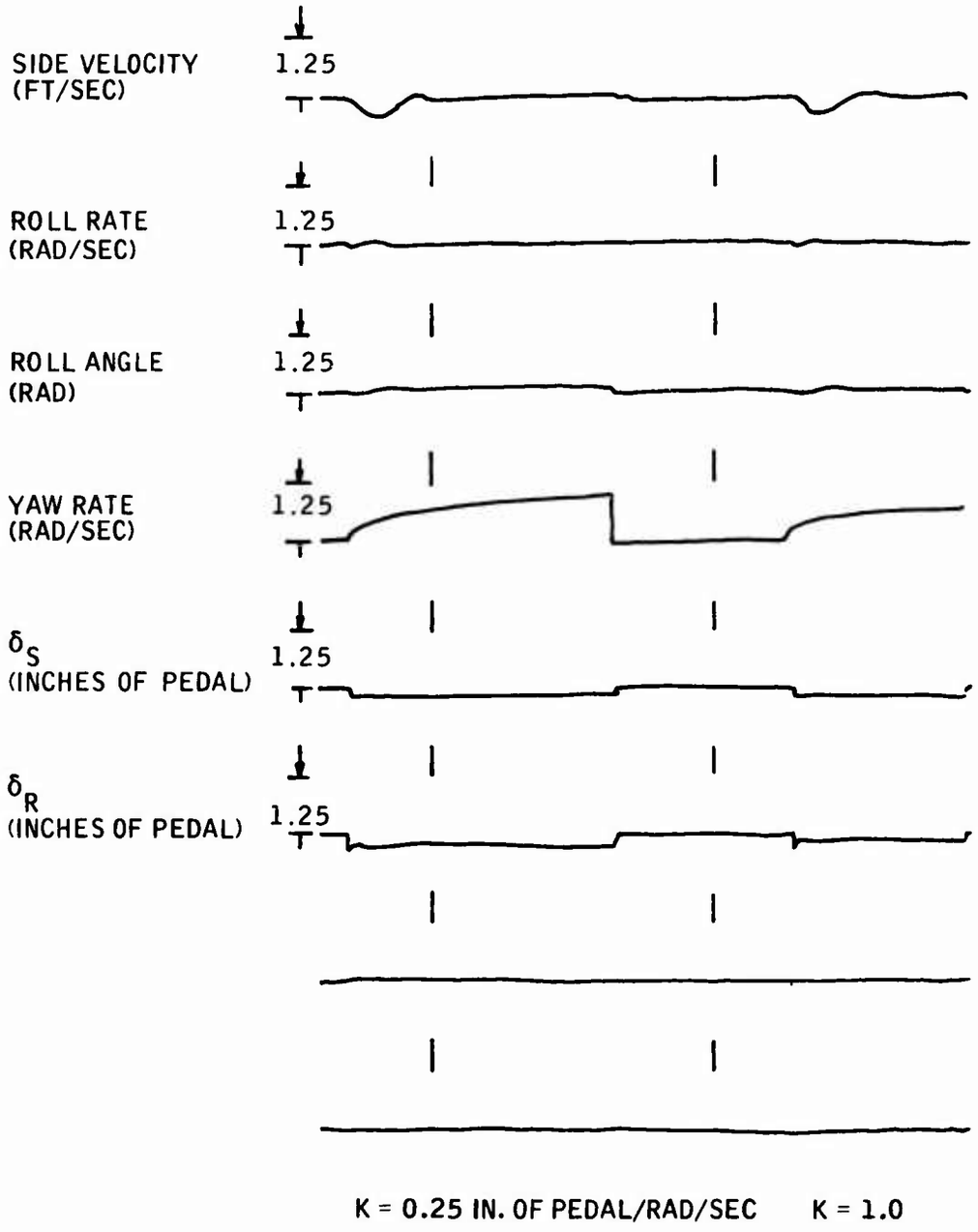

Figure 35. Straight-Through Yaw Rate With ±1/2 Rad/Sec Dead Zone - System 4 (Hover).

slowed the yaw rate divergence enough for the pilot to probably have satisfactory control, but as will be seen at 120 kn, the turn coordination suffers considerably. System 3, a straight-through yaw rate scheme, corrected the problem. For a gain of 0.25 in. of pedal/rad/sec of yaw rate (10 percent of the high-passed gain), the steady-state yaw rate is about 0.65 rad/sec, with a 0.35-in. pedal input. If the gain is doubled, yaw rate settles out at 0.45 rad/sec. It should be noted that this method is not subject to engage transients due to pedal offsets, since the straight-through yaw rate is picked off before the pedal input is summed in. Responses for system 4, using a dead zone of ±0.5 rad/sec on the straight-through yaw rate, are shown in Figure 35. This method worked satisfactorily, but is more difficult to mechanize than system 3, while offering very little in additional advantages.

The effect of each system on turn coordination was investigated using the 120 kn flight condition, as shown in Figure 36. Side velocity for a given bank angle is used as the measure of turn coordination quality. Bank angle inputs were about 35 deg. As shown in Figure 36, the free aircraft quickly achieves 0.4 ft/sec side velocity following a 35-deg bank. The nominal SAS degrades the side velocity response in that the peak overshoot is larger and settling time is somewhat longer. System 2, the 10-second high pass, degrades the turn coordination considerably, as seen in the long time required to achieve steady-state side velocity. System 3 is about the same as the nominal SAS, except that the steady-state value of velocity has increased to 0.5 ft/sec. System 4 provides the best turn coordination of all the proposed fixes. However, the turn coordination provided by system 3 is satisfactory; and in view of hardware considerations, this system should be used.

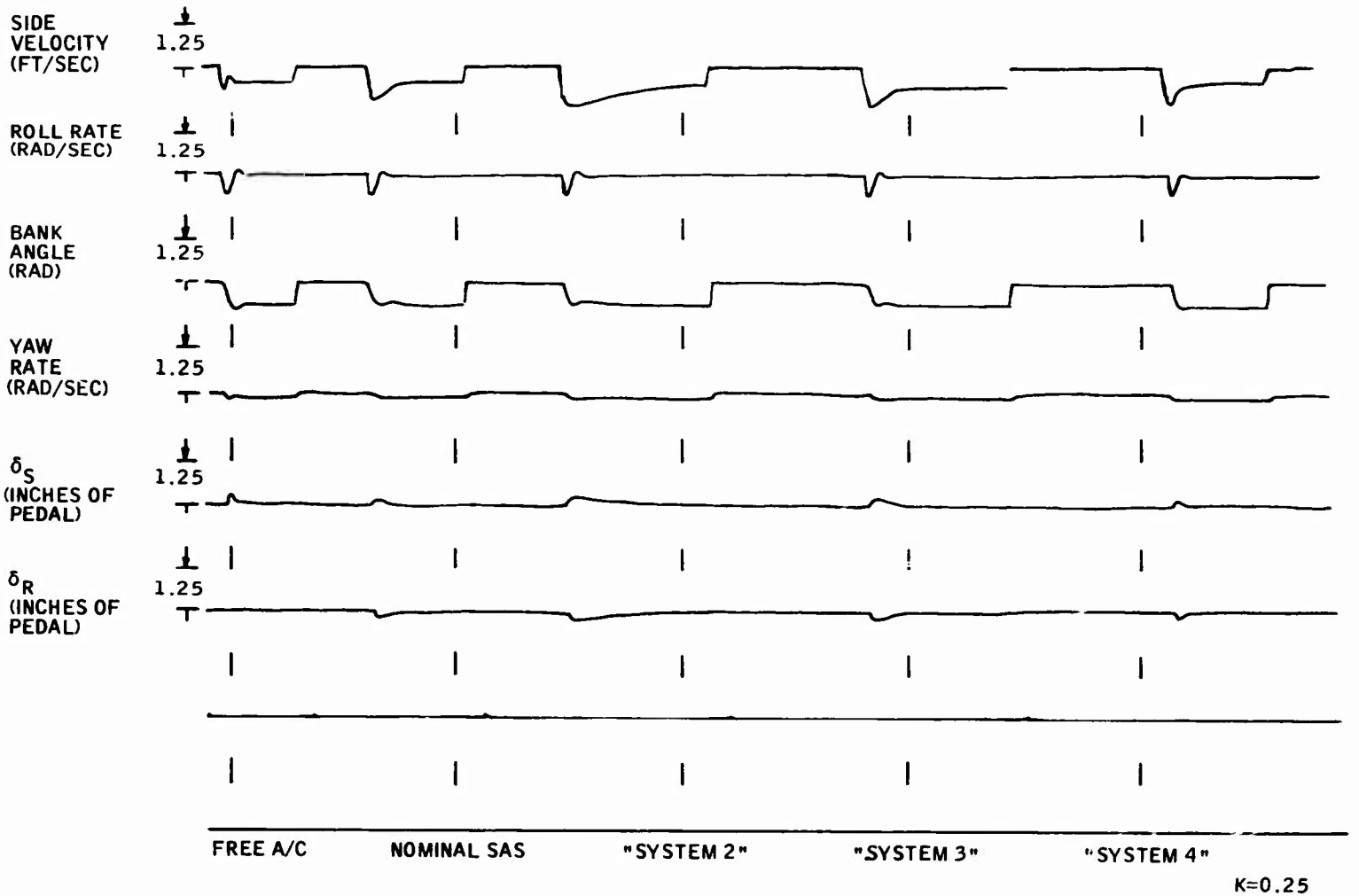

Figure 36. Turn Coordination At 120-Kn 35-Deg Bank Angle Commands.

APPENDIX II

ENVIRONMENTAL TEST PLAN FOR A
HYDROFLUIDIC SAS SUITABILITY DEMONSTRATION

Contract DAAJ02-72-C-0051

U.S. Army Air Mobility Research and Development Laboratory
Fort Eustis, Virginia

September 1973

1.0 SCOPE

This test plan defines the procedures to be followed for Environmental Testing of the YG1116A01 yaw SAS controller and servoactuator (Yaw-Axis Hydrofluidic Stability Augmentation System). The environmental tests shall consist of temperature tests, vibration tests and open-loop response tests. The unit shall operate with working fluid temperatures from 40° to 180°F.

2.0 APPLICABLE DOCUMENTS

DS 24470-01

MIL-STD-810B Environmental Test

MIL-H-5606 Hydraulic Fluid

3.0 TEST REPORTS

3.1 Test reports shall be standard Honeywell format.

3.2 DCAS witnessing will not be required for this testing.

4.0 TEST ITEM

4.1 The system shall consist of a hydrofluidic controller (YG1116A01) and a hydraulic servoactuator. See Figure 37 for schematic of system.

4.2 The system design goals shall be as listed in Paragraph 3.4 of DS 24470-01.

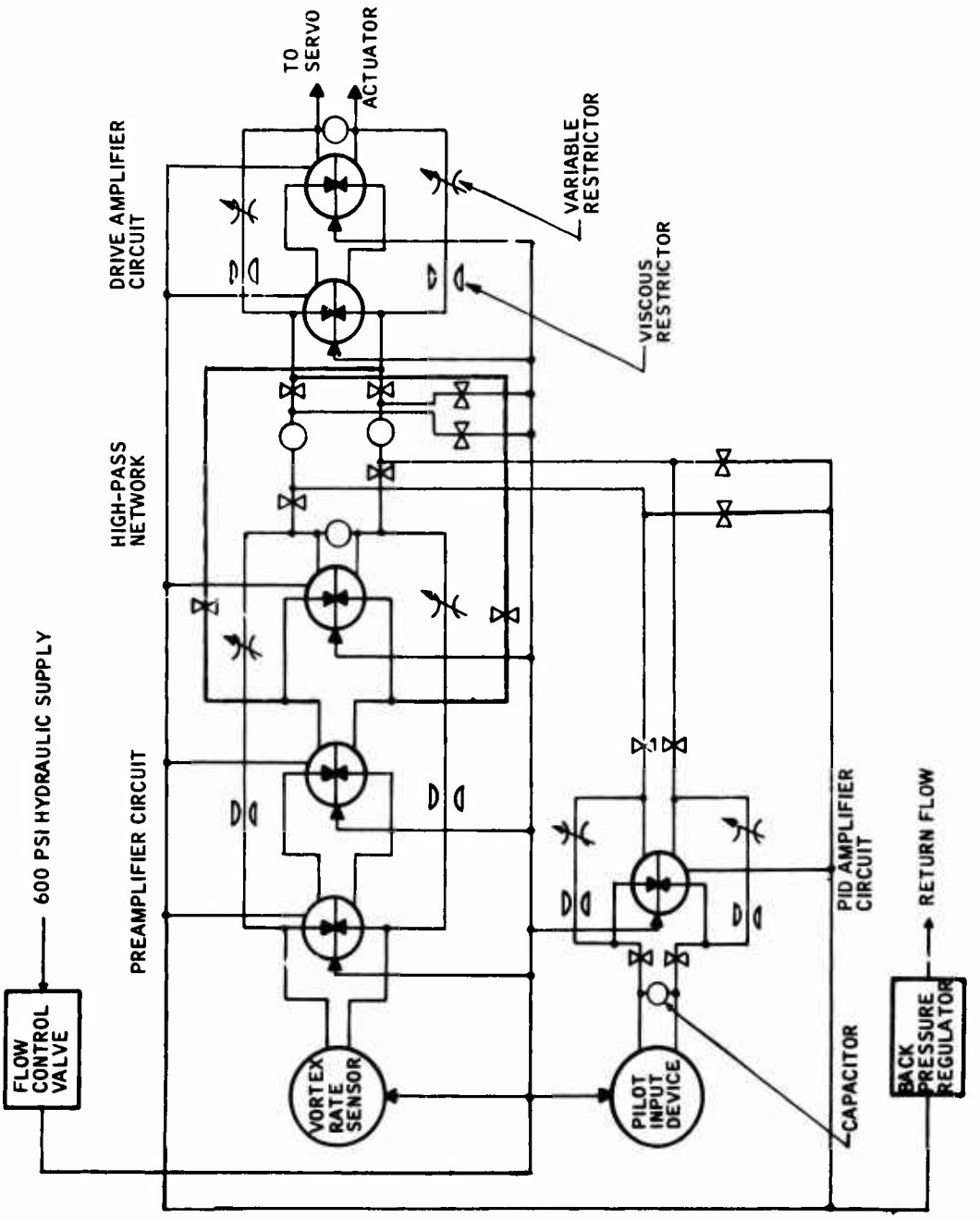

Figure 37. System Schematic.

5.0 STANDARD TEST CONDITIONS

5.1 Unless otherwise specified, all tests will be run at standard room temperature conditions (70 ± 5°F) and room barometric pressure.

5.2 Mounting - All tests unless otherwise specified, shall be conducted with the controller mounted on the servoactuator. The servoactuator will be mounted with the output axis horizontal.

All of the components comprising the system will be rigidly mounted to the test fixture. All connections, with the exception of the power supply and the two return lines, shall be with rigid tubing.

5.3 Standard Power Flow - Standard hydraulic power for the unit shall be MIL-H-5606 hydraulic fluid. The power supply shall be capable of supplying 8 $\frac{in.^3}{sec}$ at an input pressure of 600 psig. Standard fluid operating temperature will be 120 ± 5°F. All fluid flow supplied to the system will be filtered to 10 microns absolute.

6.0 TEST SCHEDULE

Environmental testing will be conducted in the following sequence:

Test	Paragraph
1. Temperature	7.0
2. Vibration	8.0
3. Open Loop Response	9.0

7.0 TEMPERATURE TESTS

7.1 The system will be mounted on the rate table in the standard configuration. The oil temperature shall be stabilized at -25°F or as cold as practical with existing equipment. A sinusoidal input rate of ±2 deg/sec at 0.4 Hz shall be applied to the system. The system shall be energized and the servoactuator motion recorded. The oil temperature shall be increased to 40°F and allowed to stabilize. The system shall be covered with a box, blanket or equivalent to reduce the temperature gradient between ambient and oil temperature. Apply sinusoidal input rates of ±2 deg/sec at frequencies of 0.01, 0.02, 0.04, 0.1, 0.2, 0.4, 1.0, 2.0, 4.0 and 10 Hz. Record the output motion of the

servoactuator. Repeat the test at the same frequencies with the input amplitude increased to ±5, ±10 and ±15 deg/sec.

Record the motion from the servoactuator with no input rate applied to the system. The total peak-to-peak noise and null of the system will meet the requirement of Paragraph 3.4.4 and 3.4.7, respectively, of DS 24470-01.

7.2 Repeat the tests of Paragraph 7.1 at oil temperatures of 70°, 90°, 120°, and 180°F.

7.3 The output of the servoactuator will meet the requirements of Figure 39 of DS 24470-01.

7.4 Apply a mechanical input to the rudder input device under the same conditions as in Paragraph 7.1 and 7.2. Total peak-to-peak motion of the input measured at the end of the control cable shall be 0.02 ± 0.005 inch. Apply frequencies of 0.01, 0.04, 0.1, 0.4 and 1.0 Hz. Record the output of the servoactuator. Repeat at amplitudes of 0.08 inch of control cable motion. The output motion of the servoactuator will meet the requirements of Figure 40 of DS 24770-01.

7.5 Rotate the BIT actuator on the controller CW. Allow sufficient time for the servoactuator motion to decay; release the BIT actuator. Record the servoactuator motion during this complete test. Repeat at each temperature.

7.6 Apply a steady rate of 10 deg/sec CW to the system while recording the output. Allow sufficient time for the servoactuator to stabilize. Remove the rate input and allow the servoactuator to stabilize. The gain shall meet the requirements of Paragraph 3.4.5 of DS 24470-01. Repeat this test in the CCW direction and also in the CW and CCW direction at a rate of 30 deg/sec. These tests shall be run at each temperature.

8.0 VIBRATION TESTS

8.1 Mount the complete system in the standard configuration on a vibration driver. The axis of the input vibration will be vertical and parallel with the rate sensor input axis. Supply the system with standard flow and pressure. The temperature of the fluid will be 120 ± 5°F.

8.2 Vibrate the complete system while it is energized and operating. The vibration amplitude and frequency shall be according to

Curve B of Figure 514-1 of MIL-STD-810B. The schedule shall be a 15-minute scan 5-500-5 Hz.

Record the servoactuator output during the complete test.

8.3 Remount the system so that the axis of vibration is parallel to the servoactuator ram axis (the rate sensor input axis still vertical). Vibrate as in Paragraph 8.2.

8.4 Rotate the system 90 deg about the rate sensor input axis and repeat Paragraph 8.2.

8.5 During all of the vibration tests, there shall be no increase in leakage from the system. There will be no line breakage or failure of fittings in the system. The maximum null shift of the servoactuator shall be no greater than 0.05 inch.

9.0 OPEN LOOP TESTS

9.1 Remount the complete system on the rate table. Energize the system and supply it with standard flow and pressure. Allow 15 minutes for the system to stabilize at 120 ± 5°F. Apply input rates of ±2 deg/sec at 0.01, 0.02, 0.04, 0.1, 0.2, 0.4, 1.0, 2.0, 4.0 and 10 Hz. Record the servoactuator outputs.

9.2 Repeat the above tests with an input of ±10 deg/sec. Record the servoactuator outputs.

9.3 The results will meet the requirements of Figure 39 of DS 24470-01.

9.4 Apply rudder inputs as described in Paragraph 7.4 Record the servoactuator output.

9.5 The results will meet the requirements of Figure 40 of DS 24470-01.

9.6 The noise and null offset recorded with no rate input will not exceed the requirements of Paragraphs 3.4.4 and 3.4.7 of DS 24470-01.

9.7 Perform the tests of Paragraph 7.5 of this document.

9.8 Perform the tests of Paragraph 7.6 of this document.

APPENDIX III

DETAIL SPECIFICATION
YAW-AXIS HYDROFLUIDIC
STABILITY AUGMENTATION SYSTEM
DS24470-01

1.0 SCOPE

This specification defines the performance requirements for the YG1116A01 Stability Augmentation System. The system is a hydrofluidic control package which mounts on top of the boost and SAS actuator of the OH-58A helicopter. This system is added to the aircraft to improve the handling qualities in the yaw axis.

The requirements of this specification are design goals.

2.0 APPLICABLE DOCUMENTS

The following documents and drawings and the applicable specifications referenced therein shall apply to the extent specified herein.

2.1 MIL-H-5606, Hydraulic Fluid, Petroleum Base, Aircraft, Missile and Ordnance.

3.0 REQUIREMENTS

3.1 General

The system shall consist of the following functional units:

3.1.1 Rate Sensor - A vortex rate sensor provides a differential pressure signal that is proportional to the aircraft angular rate in the yaw axis.

3.1.2 Amplifiers - Accept and amplify differential pressure signals.

3.1.3 Shaping Networks - Usually a combination of resistors and capacitors (bellows) designed to provide the following functions:

a) Lag - With a characteristic of $\frac{1}{TS + 1}$

b) High-pass - With a characteristic of $\frac{TS}{1 + TS}$

Note: T is a time constant.

3.1.4 Pilot Input Device - Provides an output which is a function of pedal displacement. This will reduce the tendency of the control system to "fight" the pilot in the yaw axis.

3.1.5 Servoactuator - The servoactuator, mounted effectively in series with the aircraft power boost servo, accepts differential pressure signals and converts them to displacements of the power boost servo pilot valve. Weight, bulk, and power consumption shall be optimized to the extent possible without compromising reliable and demonstrable functioning. Interunit connections shall be accomplished in a manner that will permit replacement of individual functional components.

3.1.6 Flow Control Valve - Maintain a constant flow to the system when provided a differential pressure of over 100 psid.

3.1.7 Engage Valve - Solenoid operated hydraulic valve will be remotely controlled from the cockpit to engage all or part of the control system.

3.1.8 Back Pressure Regulator - Maintains a constant return pressure level on the controller regardless of downstream pressure surges.

3.2 ENVIRONMENT

3.2.1 Vibration - A 15-minute vibration scan, with the system operating and output null monitored, will be conducted in each of the three axes at 2 g's from 20 to 500 Hz. The testing shall be conducted with the hydraulic supply and connections simulating the actual aircraft installation as near as practicable.

3.2.2 Temperature - The system shall operate over the ambient temperature range from 0 to 180°F when the operating fluid is in the range of +40°F to +180°F.

3.3 Power Supplies

3.3.1 Input power to the system shall be hydraulic fluid per MIL-H-5606 at a pressure of 600 psig (Nom) which is obtained from the aircraft hydraulic power system. The system (except augmentation servoactuators) shall not require more than $2.7 \frac{in.^3}{sec}$.

3.3.2 Electrical power for the solenoid will be 28 vdc.

3.4 System Performance

All performance requirements in this section pertain to normal operating conditions. Normal operating conditions are defined as:

- Ambient temperature - 70° ± 5°F
- Hydraulic fluid temperature - 120° ± 5°F
- Hydraulic fluid pressure - 500 to 600 psig ahead of the flow regulator; a minimum of 40 psig return pressure.

3.4.1 System requirements are summarized in Figure 38.

3.4.2 Range - The system shall have a range of at least ±30 deg/sec ahead of the high pass and ±100 percent actuator stroke downstream of the high pass.

3.4.3 Linearity - The system linearity including the servoactuator shall be within ±10 percent of full scale. Linearity is defined as the width of the band enclosing all the test points.

3.4.4 Noise - Peak-to-peak noise at output of the actuator shall not exceed ± 0.015 inch.

3.4.5 Accuracy - The system shall maintain gain and time constants within tolerances shown in Figures 39 and 40 for the high pass and pilot input loops.

3.4.6 Phasing - CCW rotation of the system shall cause the series servoactuator to retract. CW rotation of the PID cam shall cause the series servoactuator to retract (right pedal).

3.4.7 Null - the servoactuator null offset at zero input turning rate shall be no greater than ±0.07 in.

3.5 Component Performance

Performance shall be determined at room temperature ambient with fluid at 120°± 5°F, unless otherwise specified.

3.5.1 The vortex rate sensor shall meet the following performance requirements when the system is supplied with 2.7 $\frac{in.^3}{sec}$:

- Scale factor 0.014 psid/deg/sec, dead ended
- Range 30 deg/sec min

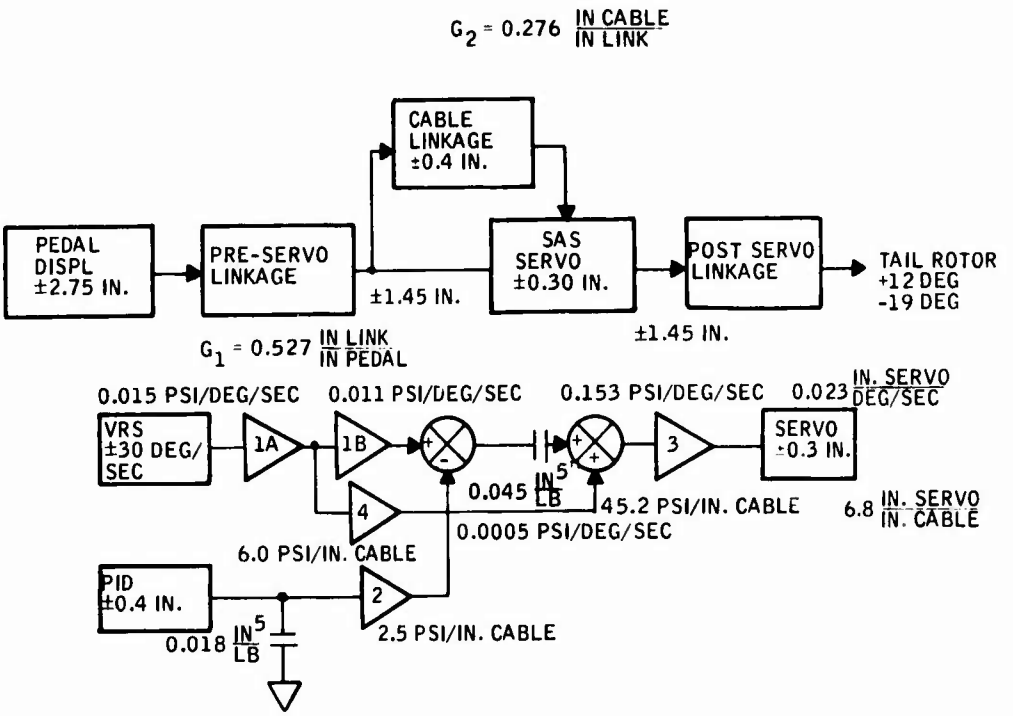

COMPONENTS

$G_{VRS} = 0.015e^{-0.06S}$ DEAD END PSI/DEG/SEC

$G_{PID} = 6.0$ PSI/IN. OF CABLE

$G_{AMP1} = 0.731$ PSI/PSI

$G_{AMP2} = 0.42$ PSI/PSI

$G_{AMP3} = 14.0$ PSI/PSI

$G_{AMP4} = 0.025$ PSI/PSI

$G_{SERVO} = 0.15 \left[\frac{(62.8)^2}{S^2 + 2(0.7)(62.8)S + (62.8)^2}\right]$ IN./PSI

$G_{CABLE} = 0.276$ IN. CABLE/IN. LINKAGE

$G_{LINKAGE} = 0.527$ IN. LINKAGE/IN. PEDAL

SYSTEM

RATE LOOP

$G_R = 0.023 \left[\left(\frac{2.5S}{2.5S+1}\right)\left(\frac{3950}{S^2 + 88S + 3950}\right)\right] e^{-0.06S}$ IN. SERVO/DEG/SEC

PID LOOP

$G_{PID} = 6.8 \left[\left(\frac{1}{S+1}\right)\left(\frac{2.5S}{2.5S+1}\right)\left(\frac{3950}{S^2 + 88S + 3950}\right)\right]$ IN. SERVO/IN. CABLE

Figure 38. System Performance (Yaw).

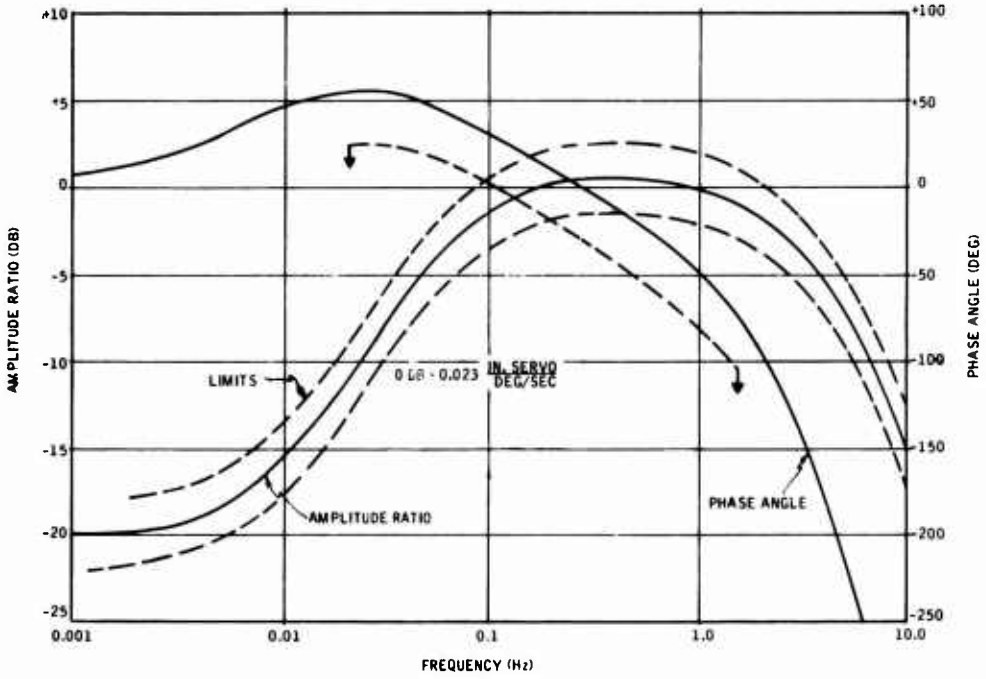

Figure 39. Rate Transfer Function Requirements.

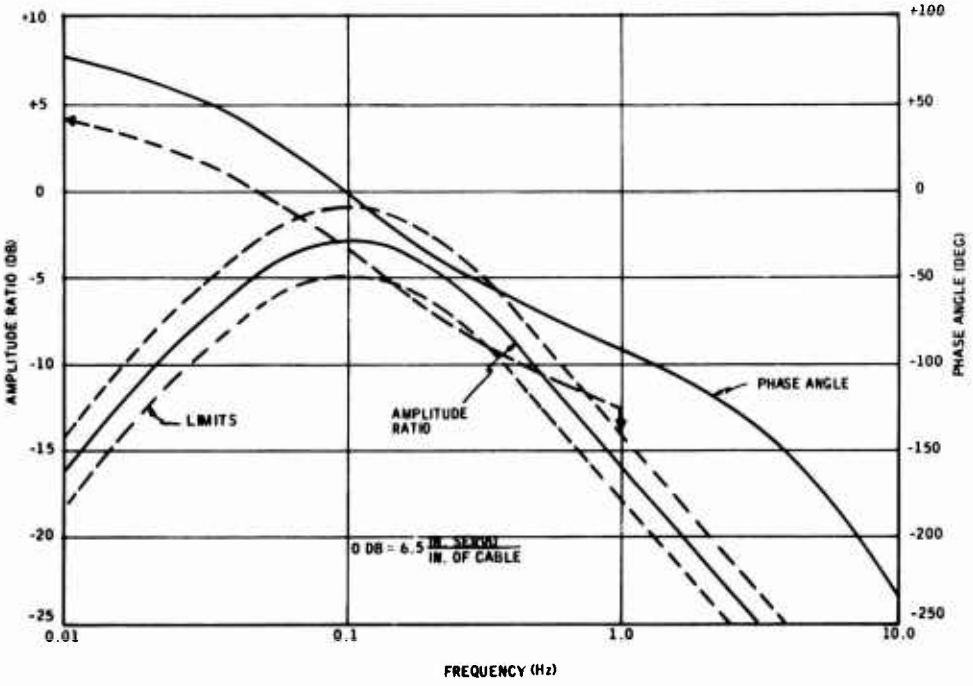

Figure 40. Pilot Input Transducer Transfer Function Requirements.

- Linearity - ± 5 percent of full scale
- Time Delay - 0.060 sec or less
- Noise - ± 0.65 deg/sec max
- Calibrate Button - A sensor calibrate button shall be utilized with the capability of inserting a signal equivalent to a step rate of about 5 degrees per second.

3.5.2 Amplifiers - Amplifiers shall meet the following performance requirements when supplied with a pressure of >6.5 psid.

- Input impedance for VRS load amplifier--180 ohms minimum
- Output impedance for output amplifier--100 ohms maximum
- Gain and load - Requirements for each application are described in Figure 38.

3.5.3 Servo - The servoactuator shall meet the following performance requirements:

Quiescent level (above R_c)	5 psig ± 1 psig
Full control signal range	± 2 psig
Max (above R_c)	15 psig
R_c Max	100 psig
Effective capacitance	<0.0005 in^5/lb
System pressure	600 psi
Stroke	± 0.300 in.
Threshold	1.0 percent max
Dynamic response	90° phase lag at 10 Hz (min) at 10 percent rated input
Linearity and hysteresis	± 5 percent of rated stroke
Inlet proof pressure	900 psi
Return proof pressure	600 psi
Burst pressure	1500 psi
Neutral leakage	0.10 gpm

4.0 QUALITY ASSURANCE

Conformance of the hardware to program objective shall be evaluated with the following tests. Performance tests will be conducted before and after vibration tests.

4.1 Vibration

4.1.1 A 15-minute vibration scan, with the system operating and output null monitored, will be conducted in each of the three axes at 2 gs from 50 to 500 Hz. The testing shall be conducted with the hydraulic supply and connections simulating the actual aircraft installation as near as practicable.

4.2 Performance Tests

4.2.1 Conformance to dynamic range requirements of Paragraph 3.4.2 shall be determined by imposing rates of ±30 deg/sec and measuring output of the appropriate stage amplifier.

4.2.2 Gain and response requirements shall be determined by measuring system output at 0.01, 0.02, 0.04, 0.1, 0.2, 0.4, 1.0, 2.0, 4.0, and 10 Hz. Amplitudes of ± 2, ± 5, ± 10 and ± 15 deg/sec shall be used. Response shall be measured with fluid temperatures of 40, 70, 90, 120 and 180°F. Results shall meet the requirements of Paragraph 3.4.

4.2.3 Gain and response of the pilot input device shall be determined by measuring system output at 0.01, 0.04, 0.1, 0.4 and 1 Hz. Amplitudes of ± 0.01 and ± 0.04 in. of cable shall be used. Response shall be measured at the same temperatures as in Paragraph 4.2.2. Results shall meet the requirements of Paragraph 3.4.

4.3 Verification

4.3.1 The systems shall be inspected for quality of workmanship and conformance to installation drawing.

4.3.2 Determine that the system contains the features described in Paragraph 3.6.1.

4.3.3 Establish that the power required does not exceed the amount specified in Paragraph 3.3.1.